COO/4268-2

PROGRESS REPORT

TO

THE UNITED STATES DEPARTMENT OF ENERGY

CONTRACT NO. EE-77-S-02-4268-A002

BIOMEDICAL RESEARCH WITH CYCLOTRON PRODUCED RADIONUCLIDES

Contract Period:	January 1, 1978 to December 31, 1978
Report Period:	October 1, 1977 to September 30, 1978

Principal Investigator	John S. Laughlin, Ph.D., Member
Co-Principal Investigator:	Richard S. Benua, M.D., Associate Member
Co-Principal Investigator:	Roy S. Tilbury, Ph.D., Associate Member
Co-Principal Investigator:	Rodney E. Bigler, Ph.D., Associate
Department:	Biophysics Laboratory 5501

SLOAN-KETTERING INSTITUTE FOR CANCER RESEARCH
410 East 68th Street
New York, New York 10021

September 30, 1978

DISCLAIMER

NOTICE

TABLE OF CONTENTS

	Page
OBJECTIVE	1
SUMMARY OF CYCLOTRON USE	1
1. METABOLIC AND TUMOR LOCALIZATION STUDIES IN MAN AND ANIMALS WITH CYCLOTRON PRODUCED RADIONUCLIDES	3
1.1. TUMOR DETECTION AND DIAGNOSIS	3
1.1.1. Design and Screening of New Radiolabeled Agents for Localizing Soft Tissue Tumors	3
1.1.2. ^{13}N-Amino Acids in Patients	10
1.1.3. ^{55}Co-Labeled Bleomycin for Tumor Localization	12
1.2. NEUROLOGICAL STUDIES	13
1.2.1. ^{13}N-Ammonia* Metabolism in Hepatic Encephalopathy	13
1.2.2. Regional Oxygen Extraction in Cerebral Ischemia	28
1.2.3. ^{15}O Gas System Modifications	31
2. RADIODRUG RESEARCH AND DEVELOPMENT	36
2.1. ^{11}C-LABELED COMPOUNDS	36
2.1.1. ^{11}C-Amino Acids	36
2.1.2. Preparation of ^{11}C-Labeled Precursors	43
2.2. ^{13}N-LABELED COMPOUNDS	47
2.3. ^{18}F-LABELED COMPOUNDS	49
2.3.1. ^{18}F-4-Fluoroestradiol	49
2.3.2. ^{18}F-Haloperidol	54
2.4. POTASSIUM-38 AS AN INDICATOR OF BLOOD FLOW TO THE MYOCARDIUM	60

Page

3. DOSIMETRY FOR INTERNALLY DEPOSITED ISOTOPES IN ANIMALS AND MAN 64

4. INSTRUMENTATION AND ANALYTICAL PROCEDURES 66

4.1. CYCLOTRON RESEARCH AND DEVELOPMENT 66

4.2. POSITRON TOMOGRAPHIC IMAGING WITH THE TOKIM SYSTEM 70

4.3. REVIEW OF POSITRON EMISSION TRANSAXIAL TOMOGRAPH INSTRUMENTS 77

5. PUBLICATIONS AND IN PRESS 81

BIOMEDICAL RESEARCH WITH CYCLOTRON PRODUCED RADIONUCLIDES

OBJECTIVE

The operation of the cyclotron has the following objectives:

(a) Research on nuclear reactions and target design for production of radionuclides.

(b) Research on labeling of biologically important compounds with cyclotron produced radionuclides.

(c) Production of radionuclides and labeled compounds for metabolic isotope research in patients and in animals carried out by the metabolic isotope study section.

(d) Development of improved cyclotron operation and beam handling technology.

SUMMARY OF CYCLOTRON USE

Table 1 is a summary of runs performed with the cyclotron during this report period. A run is used here to mean a separate request for cyclotron time, usually for several hours duration, and may include many short runs of a few minutes duration. Beam on time is the time the anode or DEE voltage was on and represents 38% of the available working hours (2006). The oscillator filament meter registered 1116 hours or 56% of the available working hours. The figures represent a slight increase over last year. A beam switching magnet would probably result in a 50% increase in beam-on time.

TABLE 1

Summary of Cyclotron Use

October 1, 1978 - September 30, 1978

Type of Run	No. of Runs	Beam on Time (Hrs.)	Use
Machine Research and Development	12		
Modifications	37		
Beam Test	16	17.5	
Operator Training	32	Included in runs listed below	
Radioisotope Production			
^{18}F	94	161.8	Bone Scanning ^{18}F Labeling
^{15}O	23	68.7	Steady-State Studies
^{11}C	38	99.0	Labeling
^{13}N	73	254.9	NH_3 Production Amino Acid Synthesis BCNU, etc.
^{52}Fe	17	40.5	Erythropoietic (Patients)
^{38}K	31	39.6	Animal Studies
^{206}Bi	2	4.9	Animal Studies
^{73}Se	3	3.1	Animal Studies
^{55}Co	1	2.5	Production Study
^{18}F Estradiol ^{18}F Haloperidol	26	44.4	Production Studies and Animals
^{43}K	1	0.9	Production Study
Miscellaneous			
Target Development	4	11.9	
Neutron Dosimetry	2	3.9	
Totals	412	753.6	

1.1 TUMOR DETECTION AND DIAGNOSIS

1.1.1. DESIGN AND SCREENING OF NEW RADIOLABELED AGENTS FOR LOCALIZING SOFT TISSUE TUMORS

OBJECTIVES

To evaluate compounds in animal tumor systems and to make a determination of feasibility for synthesis with radionuclidic labels and applicability for diagnostic imaging in cancer.

SCOPE OF INVESTIGATION

Preliminary studies were performed on the distributions of ^{14}C-tyrosine, ^{35}S-5-thio-D-glucose and ^{14}C-L-lactic acid in tumor bearing rats and mice to determine the extent of localization of activity within the tumors.

^{14}C-L-Tyrosine: A nude mouse bearing an implanted human neuroblastoma was administered (i.v.) 5 mCi of ^{14}C-L-tyrosine (uniformly labeled) and was sacrificed after six hours by exsanguination. Blood and tissue from the major organs and the tumor site were sampled. Tissue samples were solubilized and aliquots were assayed in a liquid scintillation counter. Absolute activity was determined internally in each sample with a ^{14}C-toluene standard.

^{35}S-5-Thio-D-Glucose: Paired observations were made at 24 hours of the distribution of ^{35}S activity in five tumor model systems, and a single observation was made of a sixth. Human lymphoma, human schwannoma, and human teratoma were studied in the nude mouse, colonic adenocarcinoma in the rat and Ridgeway osteosarcoma and Meth A tumor in the mouse. The animals were injected (i.p.) with 2 mCi of ^{35}S-thio-D-glucose. After 24 hours the animals were sacrificed by exanguination. Blood and tissue from the major organs were sampled. Tissues were solubilized and aliquots were assayed by liquid scintillation counting. Absolute activity was determined by the method of external standard channels ratio (ESCR).

^{14}C-Lactic Acid: A group of adult male Sprague-Dawley rats with Morris hepatoma were administered (i.v.) arbitrary amounts of ^{14}C-L-lactic acid and sacrificed at 2,10,20 and 60 minutes following administration. A minimum of four rats were studied at each time period. Blood and tissue from the major organs and tumor were sampled. Tissues were solubilized and aliquots were assayed by liquid scintillation counting. Absolute activity was determined by the method of external standard channels ratio (ESCR).

RESULTS AND CONCLUSIONS

The times at which observation of distributed activity in the cancer models were made were based upon the half-lives of nuclides with which it would have been anticipated each compound was to be labeled: ^{11}C (T 1/2 = 20 min) for L-lactic acid, ^{73}Se (T 1/2 = 7.1 hrs) for 5-thio-D-glucose and ^{18}F (T 1/2 = 2.2 hrs) for L-tyrosine. The rule of thumb applied is that the period of observation is limited to 3 to 4 half-lives because of constraints of absorbed radiation doses and photon yields. The distribution of activity in the single animal studied at 6 hrs following administration of ^{14}C-L-tyrosine did not suggest a selective uptake in neuroblastoma at this time (Table 2), although it appeared to be in excess of that seen for normal neural tissue.

The 24 hour distribution of 5-thio-D-glucose in the cancer systems are shown in Tables 3-5. Concentration in neoplastic tissue varied with tumor type and with changes in identity of host variety or species. The tumor which is seen to concentrate to the greatest extent in the McCall carcinoma and those which appear to be least effective in concentrating 5-thio-D-glucose are lymphoma, schwannoma, teratoma and Meth A. The heart and musculature are sites of heavy localization ranging from 0.2-0.5% and 4-11% of the administered dose at 24 hours, respectively. In contrast, the brain appears to effectively exclude 5-thio-D-glucose.

The distribution of activity following the administration of L-lactic acid is shown in Table 6. At 60 minutes, the highest relative concentration was found in the pancreas, followed by the liver and kidney. The tumor was only slightly higher than that of blood, while the heart was lower than blood. The estimated total body retention showed that ^{11}C was rapidly lost from the animal with only 29% remaining after 60 minutes. This was thought to be due to loss of the label, which resided at the carboxyl group, as CO_2.

These results indicate that lactic acid (^{11}C) would probably not be useful as a tumor localizing agent or as a agent for visualizing the myocardium. The results obtained with L-tyrosine and 5-thio-D-glucose do not permit such conclusions at this time. The projected use of ^{13}N and ^{11}C labels in place of ^{18}F and ^{73}Se will alter considerably the length of the observation period and interest will be focused on the early kinetics of distribution of activity following administration of these compounds.

TABLE 2

DISTRIBUTION OF ^{14}C ACTIVITY IN THE NUDE MOUSE AT 6 HOURS FOLLOWING ADMINISTRATION OF ^{14}C-L-TYROSINE

ORGAN	TISSUE/BLOOD RATIO
Pancreas	27.3
Spleen	13.7
Liver	11.9
Kidney	5.5
Tumor (Human Neuroblastoma)	2.7
Brain	2.0
Muscle	1.1
Blood	1.0

TABLE 3

RELATIVE CONCENTRATION OF ^{35}S-THIOGLUCOSE IN THE MOUSE

AT 24 HOURS FOLLOWING ADMINISTRATION

	Nude Mouse (Kennedy) Lymphoma	Nude Mouse (Kennedy) Lymphoma	AKD Mouse (Ridgeway) Osteosarc.	AKD Mouse (Ridgeway) Osteosarc.	Mouse (MethA)	Mouse (MethA)
Heart	0.339	0.854	0.741	1.29	0.308	0.394
Lungs	0.075	0.113	0.181	0.210	0.220	0.127
Spleen	0.091	0.115	0.197	0.160	0.141	0.117
Muscle	0.099	0.105	0.097	0.098	0.087	0.111
Testes	-	-	-	-	0.092	0.051
Stomach	-	-	-	-	-	-
Kidney	0.023	0.038	0.084	0.065	0.070	0.039
Pancreas	0.041	0.075	0.142	0.250	0.128	0.094
Liver	0.003	0.005	0.084	0.125	0.653	0.005
Brain	0.011	0.019	0.024	0.029	0.152	0.020
Blood	0.016	0.024	0.019	0.027	0.119	0.022
Tumor	0.037	0.055	0.211	0.228	0.112	0.037
Skin	0.033	0.090	0.148	0.167	0.113	0.086
Ovaries	0.093	0.134	-	0.177	-	
Adrenals	0.138	0.216	0.175	0.250	0.117	0.241
Fat	0.075	-	0.083	0.211	0.125	0.065

TABLE 4

RELATIVE CONCENTRATION OF ^{35}S-THIOGLUCOSE IN THE NUDE MOUSE AT 24 HOURS FOLLOWING ADMINISTRATION

Organ	Mouse 841 (Fazelli) Testic. Ca	Mouse 345 (Fazelli) Testic. Ca	Mouse 850 (Ciro) Schwannoma
Heart	0.471	1.160	0.572
Lungs	0.219	0.139	0.090
Spleen	0.157	0.137	0.092
Muscle	0.117	0.090	0.071
Testes	0.091	0.085	0.039
Stomach	0.091	0.082	0.048
Kidney	0.063	0.038	0.029
Pancreas	0.076	0.040	0.018
Liver	0.029	0.100	0.042
Brain	0.031	0.036	0.020
Blood	0.003	0.004	0.000
Tumor	0.050	0.064	0.076
Tumor	0.049	0.036	0.066
Tumor	0.031	0.031	-

TABLE 5

RELATIVE CONCENTRATION OF ^{35}S-THIOGLUCOSE IN THE RAT

AT 24 HOURS FOLLOWING ADMINISTRATION

	Buffalo Rats (McCall) Adenocarcinoma	Buffalo Rats (McCall) Adenocarcinoma
Heart	.309	.406
Lungs	.235	.350
Spleen	.484	.576
Muscles	.286	.291
Testes	.247	.075
Kidney	.323	.262
Pancreas	.058	.159
Liver	.350	.103
Brain	.261	.084
Blood	.197	.747
Tumor	.695	.583
Adrenals	.139	.177
Skin	.190	.128
Fat	.029	.100

TABLE 6

DL - LACTIC ACID - $^{14}C(1)$: RELATIVE CONCENTRATION

Tissue	Materials	2	10	30	60
Blood		2.96 ±.16	0.895 ±.070	0.648 ±.038	0.419 ±.040
Heart		1.70 ±.27	0.646 ±.068	0.513 ±.096	0.278 ±.033
Lung		2.39 ±.20	0.77 ±.17	0.566 ±.080	0.317 ±.039
Liver		3.60 ±.45	1.39 ±.07	1.25 ±.15	0.770 ±.084
Spleen		2.15 ±.10	0.765 ±.062	0.563 ±.046	0.381 ±.035
Pancreas		2.29 ±.05	1.75 ±.07	1.36 ±.09	1.18 ±.08
Small Intestine (-Contents)		2.50 ±.14	0.956 ±.067	0.716 ±.056	0.560 ±.049
Kidney		2.51 ±.32	0.91 ±.13	0.805 ±.057	0.583 ±.022
Testes		0.463 ±.028	0.592 ±.025	0.457 ±.039	0.263 ±.011
Muscle		0.462 ±.032	0.644 ±.028	0.540 ±.023	0.300 ±.023
Tumor		1.31 ±.18	1.03 ±.08	0.744 ±.063	0.507 ±.095
Skin		0.60 ±.11	0.643 ±.035	0.543 ±.050	0.252 ±.033
Calvarium		0.354 ±.004	0.308* ±.048	0.245 ±.033	0.223 ±.034
Brain		0.428 ±.073	0.407 ±.043	0.363 ±.075	0.209 ±.027
				Urine (% Dose)	0.795 ±.086

Mean ± std. error of the mean for 4 rats/ group
est. TBR (% Dose) 82 61 51 29

* 3 rats

1.1.2. ^{13}N-AMINO ACIDS IN PATIENTS

The production of ^{13}N-glutamate requires that the patient be available for imaging before the synthesis proceeds. We will report results with the new agent under several general headings by diagnosis. The dosage ranged between 1.6 and 10 mCi, and scans were begun 5 minutes after injection.

The largest group of patients to date have osteogenic sarcoma, which may be growing predominately as bone, cartilage or fibrous tissue. All are histologically proven. Ten untreated patients all had positive scans. The area of uptake corresponded to the area of the tumor rather than to the area of the destruction. One of the patients had 3 lesions; the lesion in the orbit and the pelvis were easily detected but that in the upper lumbar spine was obscured by liver uptake of ^{13}N-glutamate. The lumbar lesion was only visualized on the bone scan and confirmed by the radiograph.

Five of the osteogenic sarcoma patients had repeat scans while receiving chemotherapy but before amputation. Some showed increased uptake and some had decreased uptake in the tumor relative to the pretreatment levels. So far there is insufficient data to judge the usefulness of ^{13}N-glutamate for gauging the response to treatment.

One patient with multiple lung metastases of osteogenic sarcoma was examined with ^{13}N-sodium glutamate while receiving chemotherapy after amputation of the primary tumor. Lung metastases were present from the time of diagnosis. They were not seen in the original bone scan with diphosphonate. The lung lesions did not concentrate ^{13}N-glutamate but two of them were visualized in methylene diphosphonate bone scans on the day of the glutamate scan.

Three patients with Ewing's sarcoma in bone were examined with ^{13}N-labeled glutamate. All of the primary tumors concentrate sufficient ^{13}N to be readily identified by the scan and by computer analysis of the digital data. No patients with known metastatic Ewing's sarcoma have as yet been studied, and response to therapy has not been evaluated as yet.

A patient with recurrent nevinoma of the paravertebral region of the abdomen was evaluated with ^{13}N-glutamate. This benign tumor did not concentrate ^{13}N.

The uptake of ^{13}N-glutamate in the pancreas was outstanding. Three normal volunteers were examined and in all the pancreas was well visualized. Anterior images of the pancreas were made using the single focus collimator on the High Energy Gamma Scanner. The first volunteer was fed a light lunch 30 minutes prior to the examination. The second had a low fat lunch 90 minutes before

the scan. In the second volunteer, the pancreas counted at a higher rate than the liver. Separation of the pancreas from the liver was adequate in the second and third volunteer. The third volunteer also was imaged on the Cyclotron Corporation Positron Emission tomograph with success.

Three patients with pancreatic disease have been studied with ^{13}N-glutamate. All were fed a special luncheon 15 to 30 minutes prior to the scan to stimulate pancreatic secretion. The first patient had a cancer of the head of the pancreas on celiac angiography and on CTT examination. It appeared as a filling defect in the ^{13}N pancreas scan. The patient has subsequently died of the disease. The second patient's pancreas was not visualized presumably due to extensive carcinoma, but this remains unproven at the present time. The third patient was examined to distinguish pancreatitis from carcinoma (clinically CA, histologic biopsy was inflammation). There was poor uptake in the pancreas and it was not possible to resolve the clinical question by the ^{13}N scan.

Serial whole blood levels of ^{13}N were examined between one and 40 minutes after injection of ^{13}N in 3 subjects. The levels fell rapidly in the first 5 minutes from an initial relative concentration of 8 with a half time of about 1 minute. The relative concentration was about one at five minutes and then decreased with a half time of about one hour. The blood levels cannot be followed after 40 minutes due to physical decay. The biologic meaning of these two differing rates is not apparent at this time.

1.1.3. ^{55}Co—LABELED BLEOMYCIN FOR TUMOR LOCALIZATION

Co-55 as cobalt chloride obtained from Crocker Laboratory showed less than 1% of Co-56 and 0.1% Mn52 at the time of calibration about 12 to 20 hours before use. The purity figures were probably right judging from our analysis in the germanium detector. At 48 hours, the metal concentrations for Co, Mn and Fe were 1.2, 6.6 and 0.4 ug/ml of the original material diluted to five-fold in saline. We noted that the labeling efficiency of Co-55 bleomycin was very low. Significant free cobalt chloride was demonstrated at the site of application on the thin layer chromatograph plates. The labeling efficiency was not improved by the addition of a larger amount of carrier, adjustment of pH or longer reaction time. The tissue distribution and urinary excretion in one set of experiments are summarized as follows:

Radioactivities Recovered % of Dose at End of 21 Hours Following i.v. Injection in Female Rats, CD-Strain

	Plasma(ml)	Liver(g)	Kidney(g)	Muscle(g)	Urine (total)
Co-55 Bleo	0.012±0.001	1.28±0.11	0.78±0.09	0.027±0.001	62.5±1.1
Co-55 Cl	0.105±0.019	1.13±0.05	1.01±0.07	0.039±0.002	48.5±1.0

In contrast, tissue distribution and urinary excretion in Co-57 bleomycin and chloride showed the following figures:

Co-57 Bleo	0.010±0.003	0.114±0.031	0.359±0.058	0.004±0.001	63.6±7.75
Co-57 Cl	0.067±0.008	0.631±0.052	0.670±0.079	0.016±0.002	63.4±1.22

In nude mice with transplanted lymphoma, tumor to muscle ratio varied from 0.56 to 3.96 (0.56, 1.34, 3.41 and 3.96). In contrast, tumor to muscle in four mice given Co-57 bleomycin was 30.37±4.25 and tumor to muscle in 4 mice given Co-57 chloride was 3.72±0.57.

The reasons for the different distributions and tumor uptakes between Co-55 and Co-57 bleomycins are not clear. The possibility of contamination by divalent metals in the Co-55 preparation must be considered although our metal analysis did not substantiate such a thesis. At the present, Co-57 remains the most ideal radionuclide for labeling bleomycin.

1.2. NEUROLOGICAL STUDIES

1.2.1. ^{13}N-AMMONIA* METABOLISM IN HEPATIC ENCEPHALOPATHY

OBJECTIVE

The objective is to use ^{13}N-labeled ammonia to study the uptake mechanism and metabolism of ammonia in the brains of normal and hyperammonemic rats. This entailed the development of rapid isolation techniques for the quantitation of labeled brain metabolites, the development of surgical techniques for the infusion of isotope into cerebrospinal fluid, and the development of surgical techniques for the continuous or rapid (bolus) infusion of isotope via one common carotid artery. Understanding the metabolic fate of ammonia in the normal and hyperammonemic brain may lead to a more effective treatment for patients with liver disease.

SCOPE OF INVESTIGATION

Liver disease ranks as the sixth most common cause of death in the United States. A problem often associated with liver disease is blockage of the portal vein; the resulting pressure may cause ballooning of esophageal vessels (varisces) which if ruptured may cause GI hemorrhage and even death. Thus, a common surgical treatment involves the construction of a portacaval shunt whereby blood from the intestinal portal vein is diverted around the liver and drains directly into the systemic circulation. However, the long term survival rate of such patients is low, and the patients almost always develop neuropathological symptoms. Exactly why the brain is so sensitive to the effects of liver disease is not known. A number of substances that are known to be elevated in the plasma of patients with liver disease have been implicated as being toxic to the CNS and some are thought to act synergistically. Nevertheless, ammonia is widely regarded as the most neurotoxic agent in hepatic encephalopathy. Therefore, a detailed understanding of the metabolic fate of ammonia in the brain should provide a clue as to the causes of hepatic encephalopathy.

---

*That which we refer to as ammonia or NH_3 is, of course, a mixture of NH_4^+ ions and NH_3 gas in solution (predominantly NH_4^+ at physiological pH values). If any process upsets this equilibrium, such as depletion of NH_4^+ ions through metabolism, the equilibrium is quickly reestablished (ammonium dissociation rate constant is $\sim 3 \times 10^{10}$ sec^{-1}, and the recombination constant is $\sim 6 \times 10^5$ sec^{-1}).

Studies involving the metabolic fate of ammonia in the brain *in vivo* have been limited. ^{15}N-Labeled ammonia has been used as a tracer, but the use of ^{15}N has several drawbacks. In order to detect low levels of incorporation of label into metabolites very high concentrations of $^{15}NH_3$ have been employed with a concomitant disruption of the steady state (1). Furthermore, quantitation requires the use of a mass spectrometer which is tedious and time consuming. We have begun to use $^{13}NH_3$ to study the fate of ammonia in the brains of normal and chronically hyperammonemic rats. ^{13}N-Labeled ammonia has advantages over ^{15}N-labeled ammonia in that (a) it can be administered with a very high specific activity so that disruption of the metabolic steady state does not occur, and (b) it can be readily quantitated by means of standard radiation detectors. The main drawback with using ^{13}N as a tracer is its short half-life ($t_{1/2}$ = 10 minutes). Nevertheless, we have developed methods for the rapid isolation of labeled metabolites from the brain that involve high pressure liquid chromatography (HPLC) and chromatography on small cation and anion exchange columns that largely circumvent this limitation.

At the present time we have administered $^{13}NH_3$ to normal rats via the common carotid artery (with external carotid ligated) in order to determine the steady state distribution of ^{13}N among various brain metabolites. After ten minutes of infusion the animals were sacrificed by a "freeze-blowing" technique and the brain tissue analyzed. We have also analyzed the steady state incorporation of label into metabolites after administration of $^{13}NH_3$ via the right lateral cerebral ventricle in rats. The label was infused for 14 minutes; the rats were sacrificed by decapitation and the brains analyzed for various labeled metabolites. In both cases the overwhelming route of ammonia metabolism was found to be incorporation into the amide group of glutamine. Therefore, we also administered the glutamine synthetase inhibitor, L-methionine-SR-sulfoximine (MSO) to a group of rats, in order to determine the steady state distribution of label in the brains of rats in which glutamine synthetase activity was depleted. We have also devised a technique, modified after that of Oldendorf (2), for the measurement of the brain uptake index (BUI) of ^{13}N-ammonia relative to ^{14}C-butanol.

RESULTS

A) Distribution of Label Among Various Brain Metabolites After Administration of ^{13}N-Ammonia

1. Carotid Artery Infusion in Normal Animals. Following infusion of ^{13}N-ammonia for 10 min via the internal carotid artery, the radioactivity recovered in brain was distributed among a small number of metabolites (Table 7, Column 1). However, compared to the amount of ^{13}N-ammonia infused, the amount of label actually

TABLE 7

DISTRIBUTION OF ^{13}N AMONG VARIOUS BRAIN METABOLITES AFTER INFUSION OF ^{13}N-AMMONIA INTO RATS

METABOLITE	RELATIVE DISTRIBUTION OF COUNTS RECOVERED IN BRAIN		
	CAROTID ARTERY ROUTE NORMAL ANIMALS[1]	CEREBRAL VENTRICULAR ROUTE: NORMAL ANIMALS[2]	CAROTID ARTERY ROUTE: MSO-TREATED ANIMALS[3]
Ammonium ion	15.7 ± 2.2	33.4 ± 4.5	33.1 ± 5.3
Glutamine: α-amino group	1.0 ± 0.2	2.1 ± 0.5	2.0 ± 0.6
Glutamine: amide group	80.4 ± 1.9	59.4 ± 3.8	40.6 ± 9.3
Glutamate	0.3 ± 0.1	1.0 ± 0.4	9.8 ± 1.3
Aspartate	0.2 ± 0.1	0.6 ± 0.1	2.5 ± 0.4
Urea	1.4 ± 0.4	0.5 ± 0.1	0.8 ± 0.1
Glutathione	0.2 ± 0.1	0.3 ± 0.1	3.2 ± 0.9
Neutral amino acids (ASPN, ALA, etc.)	0.3 ± 0.1	1.2 ± 0.3	3.9 ± 0.4
γ- Aminobutyrate	0.1 ± 0.1	0.2 ± 0.2	1.5 ± 0.2
Arginine	≤ 0.1	≤ 0.1	≤ 0.1
PCA, αKGM, NAA[4]	≤ 0.1	≤ 0.1	0.9 ± 0.4
"Picric acid fraction"	≤ 0.1	≤ 0.1	1.2 ± 0.6
Insoluble Precipitate [5]	0.3 ± 0.1	0.3 ± 0.1	not determined

1 ^{13}N-Labeled ammonia (20-100 mCi) dissolved in 3 ml of physiological saline was infused into the right internal carotid artery at a rate of 0.2 ml per minute. After 10 minutes the rats were sacrificed by "freeze-blowing" the brain (n=5) or by decapitation (n=2). The distribution of label among brain metabolites was determined as described in the ERDA Progress Report E-77-S-02-4268, October, 1977, p. 22. The values obtained from the decapitated animals were not significantly different from means obtained from the "freeze-blown" animals, and the data were pooled (n=7 ± S.E.M.).

2 ^{13}N-Labeled ammonia (20-100 mCi) in 3 ml of physiological saline was infused into the right lateral cerebral ventricle at a rate of 3.4 µl per minute. After 14 minutes the animals were decapitated and the right cerebral hemisphere was analyzed for ^{13}N-labeled metabolites. The figures represent the mean from five determinations ± S.E.M.

3 As for Footnote 1, except that the animals were pre-treated with MSO (1.0 mmol/kg 3 hours before infusion of ^{13}N-ammonia. The values given are the means ± S.E.M. (n=4). The brains were removed by the "freeze-blowing"technique.

4 Abbreviations: PCA, 2-pyrrolidone-5-carboxylic acid; αKGM, α-ketoglutaramic acid; NAA, N-acetylaspartic acid.

5 A known weight of brain was homogenized in 5 volumes of 1% picric acid, centrifuged and resuspended in an equal volume of picric acid. The procedure was repeated three times and the residue counted.

recovered in the brain was low. In six animals in which the radioactivity of the whole brain was determined after infusion, the recovery of radioactivity was 4.8 ± 1.8% (S.E.M.).

Most of the label recovered in brain after intracarotid infusion of ^{13}N-ammonia was in a metabolized form (84%), of which 95% was present in the amide group of glutamine. Smaller amounts of label were detected in the α-amino group of glutamine (1%), glutamate (0.3%), aspartate (0.2%) and urea (1.4%). The relative incorporation of label into glutamate, α-amino group of glutamine and amide group of glutamine was of the order 1:3:268. Other labeled metabolites including basic amino acids, γ-aminobutyric acid, glutathione, N-acetylaspartic acid, 2-pyrrolidone-5-carboxylic acid and α-ketoglutaramic acid, combined, accounted for less than 1% of the recovered activity; approximately 0.3% was incorporated into insoluble material.

The finding of higher ^{13}N-activity in the α-amino group of glutamine compared to that of glutamate is consistent with the earlier findings of Berl et al. (1) obtained with ^{15}N-ammonia. Since glutamate is the only known precursor of glutamine and its concentration in brain is higher than that of glutamine, the greater activity in the α-amino group of glutamine is best explained by assuming that there are two pools of glutamate metabolism. Thus, blood-borne ammonia enters a small glutamate pool that rapidly turns over to glutamine; this pool is distinct from a larger pool that turns over more slowly.

2. Ventricular Infusion of ^{13}N-Ammonia in Normal Animals. Following infusion of ^{13}N-ammonia for 14 min via the right lateral cerebral ventricle, the total recovery of label in brain was 61.2 ± 6.2% (S.E.M., n=7). The labeling pattern obtained was qualitatively similar to that observed after carotid artery infusion but there were some quantitative differences (Table 7, Column 2). Thus, a greater proportion of the recovered ^{13}N-activity was unmetabolized ^{13}N-ammonia; however, of the metabolized ^{13}N-activity, most was recovered in the amide group of glutamine (89%). A higher percentage of label was incorporated into the α-amino group of glutamine, glutamate, aspartate and other amino acids than was observed after administration of ^{13}N-ammonia via the carotid artery. On the other hand, the percent incorporation into urea was lower.

As in the case of the carotid artery infusion of ^{13}N-ammonia, the ^{13}N-activity recovered in the α-amino group of glutamine after intraventricular infusion was greater than that of glutamate (Table 7, Column 2). This pattern indicates that, even though the blood-brain barrier was bypassed, ammonia entering the brain from the CSF was also metabolized predominantly in the small glutamate pool.

3. Carotid Artery Infusion in MSO-Treated Rats. In order to determine the effect of inhibition of glutamine synthetase on the distribution of ^{13}N-metabolites, rats were pretreated with MSO

and 3 hours later were infused with ^{13}N-ammonia via the internal carotid artery (Table 7, Column 3). Compared to normal animals, less of the infused radioactivity was recovered in brain (1.0 ± 0.3%, S.E.M., n=6); of the label recovered, a greater percentage was in an unmetabolized form (33%). These findings reflect the less efficient trapping of ammonia as glutamine and subsequent egress of unmetabolized ^{13}N-ammonia from brain. Nevertheless, of the label recovered in a metabolized form, a substantial amount was still found in the amide group of glutamine despite the fact that the glutamine synthetase of the whole brain was 86% inactivated. The most striking finding was that of the label recovered, the percent incorporation into glutamate was considerably greater than that in glutamine; i.e. the expected precursor-product relationship for these metabolites was obtained. Moreover, of the activity recovered in the brains of the MSO-treated animals a higher percentage was obtained in glutathione, aspartate, γ-aminobutyrate and the neutral amino acids, presumably because these metabolites either contain or are derived from glutamate.

B) Determination of Brain Uptake Index (BUI)

The BUI for ^{13}N-ammonia was determined by a modification of the technique developed by Oldendorf for the measurement of the brain uptake indices for amino acids, sugars and other small-molecular weight biochemicals (2). The technique measures the uptake of a test substance by brain, relative to that of a freely-diffusible marker; an intravascular (blood volume) marker is used to correct for incomplete washout. ^{14}C-n-Butanol was chosen as the freely diffusible marker as suggested by Raichle et al. (3); ^{111}In-DTPA was used as the intravascular marker.

The experimental design for measuring the BUI for ammonia was as follows: a cannula was placed in the right common carotid artery and led out through the underside of the neck. A Y-adapter was connected to the cannula by a short length of PE-50 tubing. One arm of the Y-adapter was attached by PE-50 tubing to a syringe containing ^{14}C-n-butanol (0.3 μCi), ^{13}N-ammonia (2 mCi) and ^{111}In-DTPA (2.5 μCi) dissolved in 0.2 ml of physiological saline. The other arm of the Y-adapter was attached to a syringe filled with heparinized physiological saline which was arranged in a Harvard infusion pump calibrated to deliver 0.2 ml/min of fluid. The two pieces of PE-50 were cut as short as possible to minimize dead space. The infusion pump was started and five seconds later the radioisotope mixture was injected as a bolus; after an additional five seconds the animal was decapitated. The brain was quickly removed; the right cerebral hemisphere was extruded through a 23 gauge needle into a liquid scintillation vial containing 2.0 ml of Protosol and the radioactivity due to ^{111}In and ^{13}N was determined in a γ-counter. After determination of γ-emitting isotopes ^{14}C-activity

was determined in a liquid scintillation counter. The brain uptake index was calculated using the following modified Oldenforf equation:

$$BUI = \left[\frac{^{13}N\text{-tissue} / ^{14}C\text{-tissue}}{^{13}N\text{-bolus} / ^{14}C\text{-bolus}} - \frac{^{111}In\text{-tissue} / ^{14}C\text{-tissue}}{^{111}In\text{-bolus} / ^{14}C\text{-bolus}} \right] \times 100$$

The brain uptake index (BUI) for ^{13}N-ammonia was 24 ± 1% (S.E.M., n=10). The fact that the BUI was substantially less than 100% indicates a considerable barrier to passage of ammonia base-ammonium ion from blood into brain. The BUI for ^{13}N-ammonia was found to be independent of concentration within the bolus over a thousand-fold range (Table 8). This concentration independence suggests that there is no carrier-mediated transport of ammonium ion across the blood-brain barrier. A similar conclusion has been reached by Phelps et al. (4) who found a constant single pass extraction for ^{13}N-ammonia in the brains of monkeys over a 17-fold range of blood ammonia concentration.

The BUI for ^{13}N-ammonia in the MSO-treated animals was similar to that obtained in the normal animals (Table 8), suggesting that the permeability of the blood-brain barrier to ammonia was not appreciably altered by MSO treatment.

TABLE 8

BRAIN UPTAKE INDEX FOR ^{13}N-AMMONIA RELATIVE TO ^{14}C-n-BUTANOL [1]

CONCENTRATION OF AMMONIA IN BOLUS (mM)	n	B.U.I. (%)
Normal animals [2]		
0.025	2	25.5, 20.1
0.59	2	20.1, 26.1
2.50	4	24.5 ± 0.4
26.0	2	25.1, 20.0
MSO-treated animals [3]		
0.03	5	26.0 ± 3.5

[1] The BUI of ^{13}N-ammonia relative to that of ^{14}C-n-butanol was determined as described in the Results Section.

[2] The specific activity of ammonia in the bolus was altered by adding either physiological saline or concentrated ammonium acetate to the ^{13}N-ammonia solution.

[3] These animals were administered MSO (i.p., 1.0 mmol/kg) 3 hours before injection of the bolus.

C) Rate of Ammonia Conversion to Glutamine within the Small Pool

Inasmuch as the glutamine synthetase reaction in the brain appears to be the major route for the metabolism of arterial-borne ammonia (Table 7), it was of interest to determine how rapidly ammonia was converted to glutamine within the small pool. Accordingly, a bolus containing ^{13}N-ammonia (20 mCi) and ^{111}In-DTPA (2.5 μCi) was injected into the right common carotid artery of normal and MSO-treated rats and five seconds later the animals were killed by the "freeze-blowing" technique. The frozen brain tissue was quickly homogenized in a 3-fold volume of ice-cold 1% picric acid and analyzed for labeled ammonia, glutamine and glutamate plus aspartate (Table 9). In the normal animals almost 60% of the radioactivity recovered in the brain had already been incorporated into glutamine (Table 9). Since the bolus takes less than 3 seconds to traverse the brain (2) and the brain is extruded 2 seconds later, one can estimate that the $t_{1/2}$ for conversion of ammonia to glutamine within the small pool is of the order 1-3 seconds.

The percent incorporation of ^{13}N-activity into glutamine was independent of ammonia concentration within the bolus up to a value (1.38 mM) at least twelve times higher than that normally found in blood (Table 9). This concentration independence implies that the concentration of ammonia in the small pool is below K_m of glutamine synthetase for ammonia. Since the concentration of ammonia in whole rat brain (181 μM; Table 10) is similar to the K_m of glutamine synthetase for ammonia (180 μM) the data also imply that the concentration of ammonia in the small pool is well below that of the brain as a whole.

In the MSO-treated animals most of the radioactivity was recovered as ammonia (Table 9). The much lower incorporation of ^{13}N-activity into glutamine presumably reflects both substantial inactivation of glutamine synthetase and greater dilution of ^{13}N-ammonia activity by endogenous brain ammonia (Table 10).

D) Metabolite Concentrations and Relative Specific Activities in "Freeze-Blown" Brain Tissue from Control and MSO-Treated Rats

The concentrations of five non-labeled metabolites in the brains of control and MSO-treated animals, infused with ^{13}N-ammonia via the internal carotid artery, are given in Table 10. The concentrations of ammonia, glutamine, glutamate, aspartate and γ-aminobutyrate in control animals are comparable to those reported previously for normal rats wherein the brains were analyzed after "freeze-blowing" (e.g. 5), or after *in situ* freezing (6). This agreement indicates that the metabolic steady state of brain was not appreciably altered by unilateral carotid ligation or by the

TABLE 9

DISTRIBUTION OF RECOVERED LABEL IN RAT BRAIN 5 SECONDS AFTER CAROTID BOLUS INJECTION OF ^{13}N-AMMONIA[1]

CONCENTRATION OF AMMONIA IN BOLUS (mM)	n	% UNMETABOLIZED	% INCORPORATION INTO GLUTAMINE	% INCORPORATION INTO GLU + ASP
Normal animal				
0.09	3	41.5 ± 1.0	57.0 ± 1.0	0.5 ± 0.2
1.38	5	41.0 ± 5.1	57.0 ± 6.2	0.5 ± 0.3
2.40	1	44.3	54.3	0.3
MSO-treated animal				
0.35	5	94.9 ± 1.7	2.5 ± 0.8	2.6 ± 0.8

[1] A bolus (0.2 ml) containing ^{13}N-ammonia and ^{111}In-DTPA in physiological saline was injected into the right common carotid artery of control and MSO-treated animals. Five seconds later the animals were sacrificed by the "freeze-blowing" technique and the brain samples were analyzed for ^{13}N-labeled metabolites as follows:

A piece of the frozen disc was homogenized in 3 vols of ice-cold 1% picric acid and centrifuged for 1 min in a Beckman microfuge. An aliquot (20 µl) of the supernate was counted for ^{13}N and ^{111}In (in order to correct for incomplete washout of ^{13}N-ammonia from the brain). Another aliquot (1 ml) was applied to the top of a Dowex 1 column (acetate, 0.5 X 2.5 cm). The pass-through and a two volume water wash were added to a Dowex 50 column (Tris, 0.5 X 2.5). The pass through and a two volume water wash from the Dowex 50 column yielded counts in glutamine; ^{13}N-ammonia was eluted with 5 ml of 1M KCl. ^{13}N-Glutamate + ^{13}N-asparatate were eluted from the Dowex 1 acetate column with 3 ml of 1M KCl.

TABLE 10

CONCENTRATIONS AND RELATIVE SPECIFIC ACTIVITIES OF VARIOUS ^{13}N-LABELED METABOLITES IN RAT BRAIN AFTER INFUSION OF ^{13}N-AMMONIA VIA THE INTERNAL CAROTID ARTERY[1]

	CONCENTRATION mmol/kg Wet Weight			^{13}N-SPECIFIC ACTIVITIES NORMALIZED TO CONTROL GLUTAMINE AMIDE [2]		
METABOLITE	Controls (n = 12)	MSO-Treated (n = 5)	p	Controls (n = 4)	MSO-Treated (n = 4)	p
Glutamine: Amide Group	5.84 ± 0.23	4.87 ± 0.21	< 0.02	[100 ± 29]*	8.0 ± 2.β*	0.028
Glutamine: α-amino Group				1.2 ± 0.4*	0.6 ± 0.2*	N.S.
Glutamate	10.35 ± 0.40	9.24 ± 0.81	N.S.	0.26 ± 0.07	1.4 ± 0.2	0.028
Aspartate	2.89 ± 0.08	2.19 ± 0.09	< 0.002	0.56 ± 0.14	1.4 ± 0.56	N.S.
γ-Aminobutyrate	1.49 ± 0.06	1.39 ± 0.07	N.S.	0.56 ± 0.26	0.90 (n = 3)	N.S.
Ammonia	0.181 ± 0.014	0.818 ± 0.098	< 0.002	-----	-----	
Ammonia (arterial blood)	0.107 ± 0.033 (n = 3)	0.295 ± 0.033 (n = 8)	< 0.02			

[1] Rats were infused with physiological saline containing ^{13}N-ammonia via the internal carotid artery as described in the text. After 10 min the brains were removed by the "freeze-blowing" technique. Significance was determined by using the Two-tailed Mann-Whitney U Test.

[2] Values were determined only on those samples in which the frozen tissue was analyzed both for metabolites and for ^{13}N. The specific activities were calculated by taking into account the known recovery of radioactivity per brain. The average total recovery of counts within the brain for each metabolite (± S.E.M.) was divided by the concentration of that metabolite; the glutamine (amide) value for the control group was arbitrarily assigned a value of 100. The large standard errors of the means are due in part to the fact that the percent recovery of ^{13}N-activity in the brain, relative to the injected dose of ^{13}N-ammonia, varied from 2.3 to 9.3% in normal animals and from 0.4 to 1.6% in MSO-treated animals.

* Different from glutamate values within the same column with p=0.028.

infusion of isotope. In the MSO-treated animals ammonia concentrations increased three-fold in the blood; this was accompanied by a five-fold increase in the brain ammonia level. In the brains of MSO-treated rats there were also small but significant decreases in the concentrations of glutamine, aspartate and possibly glutamate ($p < 0.1$) compared to the controls (Table 10). Reduction of brain glutamine following MSO treatment of rats was previously reported by Folbergrova (7).

The higher incorporation of ^{13}N-activity into the α-amino group of glutamine compared to that of glutamate (Table 7) was also true of the ^{13}N-specific activities for control animals. Thus, the relative specific activities of glutamate, α-amino group of glutamine, and amide group of glutamine were 1:4.6:385, respectively. On the other hand, in animals given MSO, the ^{13}N-specific activity of glutamate was greater than that for the α-amino group of glutamine; the relative specific activities of glutamate, α-amino group of glutamine, and amide group of glutamine were of the order 1:0.44:5.9 (Table 10). Compared to controls, the specific activity of the amide group of glutamine decreased by a factor of twelve in the MSO-treated animals, whereas the specific activity of glutamate increased by a factor of five (Table 10). A reasonable explanation for the decrease in the specific activity of glutamine (amide) is the considerable inactivation of glutamine synthetase in the small pool coupled with a dilution of ^{13}N-ammonia in the small glutamate pool. Because the combined specific activity of glutamate plus glutamine (α-amino) was twice the control value and the concentration of ammonia was six times greater than controls, the rate of synthesis of ^{13}N-glutamate from ^{13}N-ammonia must have increased at least 12-fold in the MSO-treated animals. These data indicate that the two pools of glutamate metabolism are no larger metabolically distinct in the brains of MSO-treated animals.

CONCLUSION

Nitrogen-15 has been used as a biological tracer for about forty years. Schoenheimer and colleagues, in a series of experiments, administered ^{15}N-ammonia or ^{15}N-labeled amino acids to rats and were the first to demonstrate that nitrogen derived from ammonia was incorporated into urea, the amide group of glutamine, other amino acids and creatine (cf. 7). It had originally been assumed that deamination of L-amino acids *in vivo* was accomplished by the consecutive action of a specific α-ketoglutarate-dependent transaminase and glutamate dehydrogenase (8) and that incorporation of ^{15}N, derived from ^{15}N-ammonia, into amino acids occurred by the reversal of this reaction. However, Duda and Handler showed that although ^{15}N-ammonia was incorporated into amino acids, the major fate of ^{15}N, whether administered intravenously as ^{15}N-ammonia or derived from endogenously produced ^{15}N-ammonia (as in the breakdown of D-^{15}N-leucine), was incorporation

into the amide group of glutamine (9). This labeling pattern was found to hold for liver, kidney, brain and other tissues. Later, Berl et al. (1) on the basis of labeling patterns obtained after intracarotid administration of ^{15}N-ammonia to cats, postulated the existence of at least two distinct compartments of ammonia metabolism in brain. Thus, although glutamate is the only known precursor of glutamine, the specific activity of ^{15}N-labeled glutamate was found to be lower than that of the α-amino and amide groups of glutamine (1). It was postulated that in the brain, blood-borne ammonia enters a small glutamate pool that is both rapidly turning over and distinct from a larger glutamate pool.

In the present study we have utilized ^{13}N-ammonia to investigate the cerebral uptake and metabolism of ammonia in conscious rats. The findings indicate that under physiological conditions cerebral ammonia metabolism occurs in at least two compartments, in agreement with the previous postulate of Berl et al. (1). The recent work further shows that: 1) ammonia enters the brain largely by diffusion, 2) the glutamine synthetase reaction of the small pool is the overwhelming route for the detoxification of blood-borne and CSF-borne ammonia in the brain; the glutamate dehydrogenase reaction is <1% as effective as the glutamine synthetase reaction, 3) the conversion of ammonia to glutamine within the small pool is exceedingly rapid, 4) methionine sulfoximine strongly inactivates the small pool glutamine synthetase, so that the small pool can no longer efficiently trap blood-borne ammonia; blood-borne ^{13}N-ammonia mixes with the large pool ammonia where it is is available for the synthesis of ^{13}N-glutamate, i.e. the expected precursor-product relationship between glutamate and glutamine (α-amino group) obtains. Figure 1 is a schematic diagram of the routes of arterial-borne ^{13}N-ammonia metabolism in the brains of control rats, and of animals that were pretreated with methionine sulfoximine.

Berl et al (1) have speculated that newly-synthesized glutamate may be amidated in the mitochondria before mixing with other tissue pools of glutamate. However, the present work would seem to rule out a mitochondrial localization for the small pool. If the mitochondria represented the small pool and the soluble fraction represented the large pool, then in order to account for the finding that after MSO-treatment the specific activity of glutamate was five times greater than controls, one would have to postulate that the soluble fraction contained far more glutamate dehydrogenase activity than the small pool. However, this is an unreasonable assumption since brain glutamate dehydrogenase is known to be almost exclusively mitochondrial. We believe that the small and large pools are cellular compartments and that the small pool is juxtaposed between the blood-brain barrier (or in the case of the CSF, the ependyma) and the large pool.

There is much indirect evidence from ^{14}C-labeling patterns, obtained after incubating brain slices with ^{14}C-γ-aminobutyrate and ^{14}C-glucose, that astrocytes constitute at least part of the

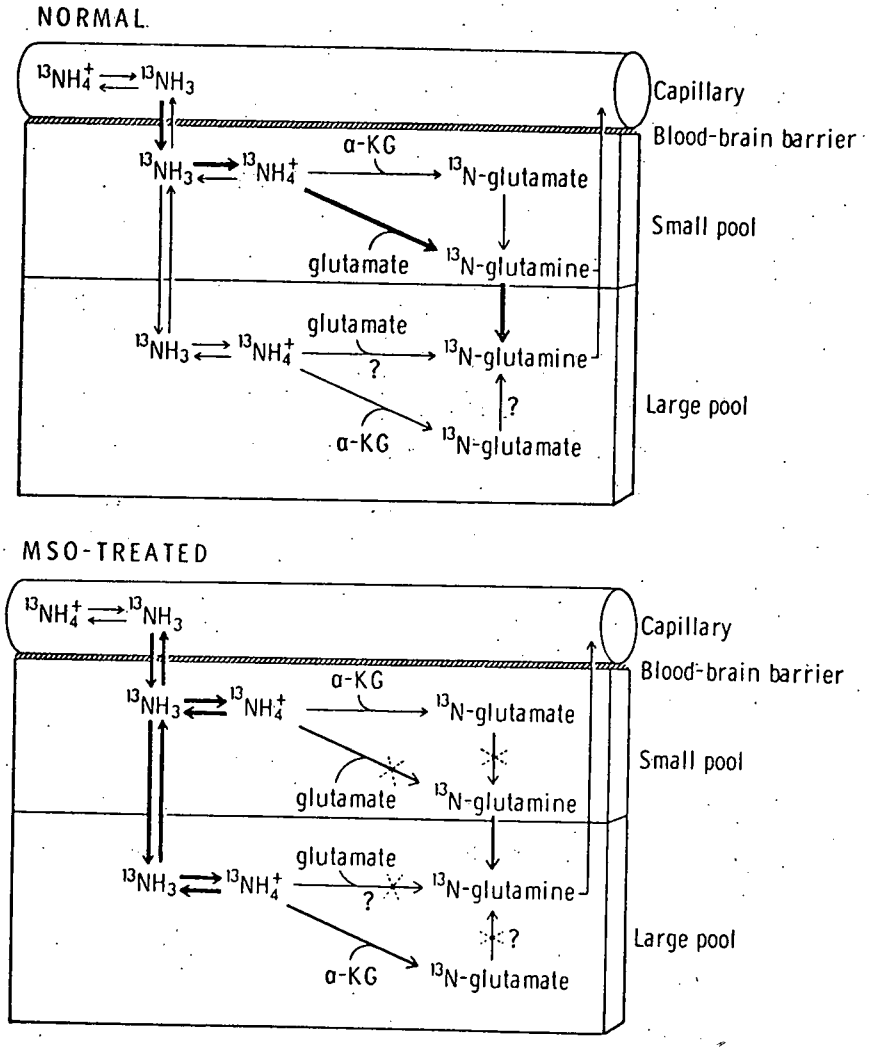

Routes of arterial-borne ^{13}N-ammonia metabolism in the brains of normal and MSO-treated animals. ^{13}N-Ammonia enters the small compartment by diffusion of the free gas. In the normal animal the major route of metabolism is via a reaction with glutamate to yield amide labeled glutamine (> 96%) with a $t_{1/2}$ of 1-3 sec; a very small amount crosses into the large pool, is lost to the arterial blood or is incorporated into glutamate within the small pool (< 4%). In the MSO-treated animal the glutamine synthetase of the small pool is largely inactivated so that a considerable portion of ^{13}N-ammonia entering the small pool may diffuse back into the arterial circulation or diffuse into the large pool; some of the ^{13}N-ammonia, however, is trapped as ^{13}N-glutamate and ^{13}N-glutamine within the small pool. Much of the ^{13}N-ammonia entering the large pool is incorporated into ^{13}N-glutamate. The question marks on the figure have been added to indicate that, at the present time, it is not certain whether or not the large pool possesses glutamine synthetase activity. The relative importance of the various pathways is indicated by the thickness of the arrows. The broken-line crosses indicate sites of possible MSO inactivation of glutamine synthetase.

small pool and neuronal structures contribute to the large pool (11). Moreover, the astrocytes are morphologically in the right place. Foot processes of astrocytes surround the brain capillaries, and thus constitute an integral part of the anatomical blood-brain barrier; distally, astrocytes abut onto neurons. Furthermore, Martinez-Hemandez et al. have demonstrated by an immunohistochemical technique that much of the glutamine synthetase activity of the brain is confined to glial cells, being particularly rich in the peri-vascular astrocytes (12).

In addition to providing a structural matrix for the neurons, glial cells appear to exert a homeostatic influence upon the neuronal interstitial environment. Thus, glial cells have long been recognized as important regulators of the extracellular potassium ion concentration in brain (13); they also possess saturable, high-affinity uptake systems for the transport of glutamate (14), γ-aminobutyrate (15), and a variety of other putative neurotransmitters including dopamine, norepinephrine and serotonin (16). Moreover, glial cells contain virtually all of the carbonic anhydrase activity of the brain (17). Inasmuch as they also appear to contain most of the brain glutamine synthetase activity, glial cells may play a pivotal role in the elimination of the major end-products of cerebral metabolism, namely, carbon dioxide and ammonia.

REFERENCES

1. Berl, S., Takagaki, G., Clarke, D.D., and Waelsch, H. Metabolic compartments *in vivo*. J. Biol. Chem. 237:2562-2569, 1962.

2. Oldendorf, W.H., and Braun, L.D. (^{3}H)-tryptamine and ^{3}H-water as diffusible internal standards for measuring brain extraction of radio-labeled substances following carotid injection. Brain Research 113:219-224, 1976.

3. Raichle, M.E., Eichling, J.O., Straatman, M.G., Welch, M.J., Larson, K.B. and Ter-Pogossian, M.M. Blood brain barrier permiability of ^{11}C-labeled alcohols and O-water. Blood flow and metabolism (Harper, M., Jennet, B., Miller, D., and Rowan, J., Eds.) pp. 7.11-7.14, Churchill Livingstone, New York, 1975.

4. Phelps, M.E., Hoffman, E.J., and Raybaud, C. Factors which affect cerebral uptake and retention of $^{13}NH_3$. Stroke 8:694-703, 1977.

5. Hawkins, R.A., Miller, A.L., Nielsen, R.C., and Veech, R.L. The acute action of ammonia on rat brain metabolism in vivo. Bio. Chem. J. 134:1001-1008, 1973.

6. Hindfelt, B., Plum, F., and Duffy, T.E. Effect of acute ammonia intoxication on cerebral metabolism in rats with partacaval shunts. J. Clin. Invest. 59:386-396, 1977.

7. Folbergrová, J. Free glutamine level in the rat brain *in vivo* after methionine sulfoximine administration. Physiol. Bohemoslov. 13:21-27, 1964.

8. Schoenheimer, R. The dynamic state of body constituents. Harvard University Press, 1942.

9. Braunstein, A.E., and Bychkov, S.M. A cell-free enzymatic model of ℓ-amino-acid dehydrogenase (ℓ-Deaminase). Nature (London), 144:751-752, 1939.

10. Duda, G.A., and Handler, P. Kinetics of ammonia metabolism in vivo. J. Biol. Chem. 232:303-314, 1959.

11. Balázs, R., Machiyama, Y., Hammond, B.J., Julian, T., and Richter, D. The operation of the γ-aminobutyrate bypath of the tricarboxylic acid cycle in brain tissue in vitro. Biochem. J. 116:445-467, 1970.

12. Martinez-Hernández, A., Bell, K.P., and Norenberg, M.D. Glutamine synthetase: Glial localization in brain. Science 195:1356-1358, 1976.

13. Henn, F.A., Haljame, H., and Hamburger, A. Glial cell function: Active control of extracellular K^+ concentration. Brain Res. 43:437-443, 1972.

14. Hertz, L., Schousboe, A., Boechler, N., Mukerji, S., and Federoff, S. Kinetic characteristics of the glutamine uptake into normal erythrocytes in culture. Neurochem. Res. 3:1-14, 1978.

15. Hutchison, H.T., Werrbach, K., Vance, C., and Haber, B. Uptake of neurotransmitters by clonal lines of astrocytoma and neuroblastoma in culture. 1. Transport of γ-aminobutyric acid. Brain Res. 66:265-274, 1974.

16. Henn, F.A., and Hamberger, A. Glial cell function: Uptake of transmitter substances. Proc. Natl. Acad. Sci. USA, 68: 2686-2690, 1971.

17. Giacobini, E. Localization of carbonic anhydrase in the nervous system. Science 134:1524-1525, 1961.

1.2.2. REGIONAL OXYGEN EXTRACTION IN CEREBRAL ISCHEMIA

OBJECTIVE:

This is an investigation utilizing cyclotron-produced oxygen-15 labeled gases to assess changes in brain metabolism and blood flow caused by transient cerebral ischemia. The underlying hypothesis is that transient cerebral ischemia may cause a secondary disruption of the normal coupling between brain blood flow and metabolism. The specific question to be answered is whether blood flow falls at a time of increased metabolic need, a situation that could produce additional ischemia and thus secondary brain damage. The techniques being developed for this study will ultimately be applicable to human stroke since they are minimally invasive and might in time prove useful in assessing the course and effects of therapy in individual patients.

SCOPE OF INVESTIGATION:

As it will take a number of years for all aspects of the general objectives to be met, steps to be completed in each year have been formulated. The first aim is to develop techniques that will permit a comparison of cerebral blood flow and metabolism determinations, as derived from the ^{15}O-gas continuous inhalation model suggested by Jones, et al. (1) and described in further detail recently by Subramanyam, et al. (2), with standard results derived from Kety-Schmidt CBF and A-V oxygen difference measurements. Since this phase involves measurement of whole brain blood flow and oxygen metabolism, the following goals were set:

(a) Acquire standard techniques for measuring blood flow and metabolism.

(b) Adapt imaging instruments and supporting equipment for the imaging of monkey and baboon brains during inhalation of ^{15}O-labeled gases.

(c) Simultaneous development of a model of regional brain ischemia in baboons and cynomologous monkeys, to be introduced after the validation of the ^{15}O blood flow and metabolism techniques.

RESULTS AND CONCLUSIONS:

No complete animal studies were performed during this past year with the ^{15}O-gases O_2, CO_2 and CO due to our inability to consistently supply these gases in a quality suitable for inhalation, and to rapidly convert between the production of the

three gases. The steps that have been taken to rectify this situation are detailed in Section 1.2.3 of this report.

It was demonstrated that satisfactory 2-dimensional brain images, with good depth independence and 1 cm spatial resolution, could be obtained utilizing our High Energy Gamma (HEG) rectilinear scanner in the β^+ coincidence mode of operation (resulting image is conventional 2-dimensional projection, not tomographic reconstruction), for the ^{15}O-labeled gases administered by continuous inhalation to a paralyzed, ventilated baboon. The digital data contained in these ^{15}O images can be quantitated and used for the global, and subsequent hemispheric, determinations of cerebral blood flow and oxygen metabolism being evaluated. Computer programs used to display and quantitatively analyze these image data include edge-finding algorithms to define organ (e.g. brain) boundaries, a number of filtering and re-focusing options, and the capability of producing composite images of two or more original images mathematically combined in various ways (e.g. an O_2/CO_2 quotient image representing oxygen extraction).

The standard methods to be used in determining cerebral blood flow and oxygen utilization is the xenon-133 method developed here by Gjedde et al. (3). Dr. Levy has acquired this technique in small laboratory animals (rats) so that it can subsequently be applied to baboons or monkeys. Also, Dr. Levy has developed a regional cerebral blood flow method that could be applied to baboons undergoing oxygen-15 studies. This is a modification of Goldman and Sapirstein's (4) indicator-fractionation technique that utilizes ^{14}C-butanol. Though developed primarily for small laboratory animals and despite the fact that the method requires sacrifice of the animal, it could be used after an oxygen-15 determination to obtain an independent measure of regional cerebral blood flow.

Some progress has also been made in preparing for experiments on regional brain ischemia. Dr. Brierley in England has prepared 6 baboons subjected to unilateral common artery occlusion and systemic hypoxia. All of these have been spontaneously-breathing baboons, and cardiorespiratory collapse intervened before any brain damage developed. Dr. Levy at Cornell has produced unilateral common carotid artery occlusion and systemic hypoxia in one mechanically-ventilated, unanesthetized baboon. Though focal EEG abnormalities developed, the brain of this animal showed no morphological abnormalities. Additional experiments involving longer and more profound hypoxia are planned. Consideration is also being given to a second animal model for regional brain ischemia; this would use the cynomologous monkey (macaca irus) and a much more invasive surgical technique to perform cerebral artery occlusion. This could be used as an alternate cerebral ischemia model; while not as large as the baboon's brain, the cynomologous monkey's brain (at 60-80 g) is

still large enough to be useful in our 2-dimensional imaging studies on the global or hemispheric scale, and for studies using β^+ emission tomography.

REFERENCES

1. Jones, T., Chesler, D.A., and Ter-Pogossian, M.M. The continuous inhalation of oxygen-15 for assessing regional oxygen extraction in the brain of man. Brit. J. Radiology 49:339-343, 1976.

2. Subramanyam, R., Alpert, N.M., Hoop, B., et al. A model for regional cerebral oxygen distribution during continuous inhalation of $^{15}O_2$, C^{15}O, and C$^{15}O_2$. J. Nucl. Med. 19:48-53, 1978.

3. Gjedde, A., Caronna, J.J., Hindfelt, B., and Plum, F. Whole-brain blood flow and oxygen metabolism in the rat during nitrous oxide anesthesia. Am. J. Physiol. 229:113-118, 1975.

4. Goldman, H. and Sapirstein, L.A. Brain blood flow in the conscious and anesthetized rat. Am. J. Physiol. 224:122-126, 1973.

1.2.3. O-15 GAS SYSTEM MODIFICATIONS

OBJECTIVE

To improve the system for producing O-15 labeled gases so that they may be delivered at constant radioactive concentration, and may be changed rapidly from one radioactive gas to another.

SCOPE OF INVESTIGATION

In December 1977 after several experiments were not completed due to inadequacies of the specifications of the ^{15}O gases supplied, and due to long times required to change from one gas to another, it was decided to modify the gas system to eliminate these problems. In addition, the implementation of a technique for the detection of left to right cardiac shunt (1,5) with $C^{15}O.O$ required a very high radioactive concentration.

The primary use of gases labelled with ^{15}O at SKI is the study of regional oxygen metabolism in cerebral ischemia (2). These experiments involve sequential administration of $^{15}O.O$, $C^{15}O.O$, and $C^{15}O$ (in any order) to a paralysed, non-anesthetized baboon held in a positioning jig in the imaging device. The amount of the paralytic drug which can be administered and the number of times it can be used in a given experiment is limited; too much drug causes death of the experimental animal. The time required to change from one ^{15}O labelled gas to another was about 20 to 30 minutes. The radioactive gas supply system has been functional and virtually unchanged since its assembly in 1969 (3). Changing gases with this system required shutting off the cyclotron beam, allowing the radioactivity in the vault to decay to a safe level, entering the cyclotron vault, and manual manipulation of tubing with quick disconnect endings. After reclosing the vault, restarting the cyclotron and fine tuning the beam, the radioactive gases required from 15 to 45 minutes to reach constant levels of gas flow and radioactive concentration (steady state). The long time required to reach steady state was due to the use of large volume cannisters for containing reagents in the process line (E.G. Drierite, Baralyme). Once steady state was obtained, the amount of breathing or diluting gas needed to make the radioactive gas suitable for administration was calculated and added. This disturbed the flow of target gas and required additional waiting while the system again stabilized. The use of $C^{15}O$ as a label for blood in the determination of cerebral blood volume demands the total concentration of CO be $\leq$ 50PPM in the administered gas to avoid any toxic effect. It was very difficult to meet this requirement with the original system.

The use of $C^{15}O.O$ in cardiac shunt studies involves a single breath administration of the gas which must contain sufficent activity to accomplish the study. To achieve the maximum

concentration of $C^{15}O.O$ in the target gas and maintain this level ready for demand use, it was decided to install a pump and return line to allow recirculation of the gas through the target.

RESULTS AND CONCLUSIONS

A diagram of the system as modified is shown in Figure 2. The 2-way solenoid valves in the target room used to control the flow of various target gases are operated through the Process Equipment Remote Control Systems (PERCS) (4). This allows the remote selection of any combination of four primary (target) gases in cylinders I through IV at preset flow rates for supply to the target chamber through flowmeters in the target room. From the target chamber the irradiated gas flows to processing apparatus in the cyclotron vault. Three way solenoid valves on the input and output sides of each process train (1A through 3B, Figure 2) enable flushing the processing train with a non-reactive gas while maintaining them ready for use at temperature under flowing conditions. The target gas is led to each train, but does not flow until the three-way solenoid valves are set by operating switches in the hot lab. Each set of valves (A & B) are connected to operate together from one switch. From the processing train the gas is led through about 100 feet of tubing to the warm lab, for analysis, dilution, and use. The containers for baralyme, drierite, and activated charcoal were changed from the original 3" ODX 12" long glass cannisters to 1/2" ODX 12" long copper tube, reducing the internal volume by a factor of 30. All of the original 0.250" ODX 0.045" wall accessible plastic tubing was replaced with 1/8" ODX 0.030" wall copper tubing. The output flow in the warm lab was stabilized by the installation of a Brooks Model 8944A flow controller, providing a constant flow gas independent of pressure variations down stream from the controller.

These modifications allow changeover between $^{15}O.O$ to $C^{15}O.O$ by toggle switch operation. The cyclotron remains on during the change. Conditions of constant flow and constant radioactive concentration are reached within four minutes. At a gas flow of about one liter per min., 5 μAmp of 7.8 MeV deuterons on target resulted in the delivery of 48.5 mCi $^{15}O.O$/liter of gas (N_2). A flow of 0.8 liter/min and 10 uA beam current the yield was 27 mCi $C^{15}O.O$/liter of gas (N_2). The target gas for both $^{15}O.O$ and $C^{15}O.O$ is 1% oxygen, balance nitrogen. To reduce the total CO concentration of the $C^{15}O$ the oxygen in the target gas was reduced to 0.01%. Some carrier oxygen must be present in the target gas or most of the ^{15}O produced remains in the target chamber, probably through exchange with residual oxygen in the target chamber material (aluminum). The target gas is diluted about 5:1 with breathing air and oxygen for administration. By holding the target gas oxygen to 0.01%, the CO concentration is held correspondingly low. Oxygen-15 labelled CO has been prepared for administration with a concentration of 1.5 mCi $C^{15}O$/litre/min. Target gas flow was 0.9 l/min. Radiochemical purity was 99%.

FIGURE 2 SKI GAS HANDLING SYSTEM

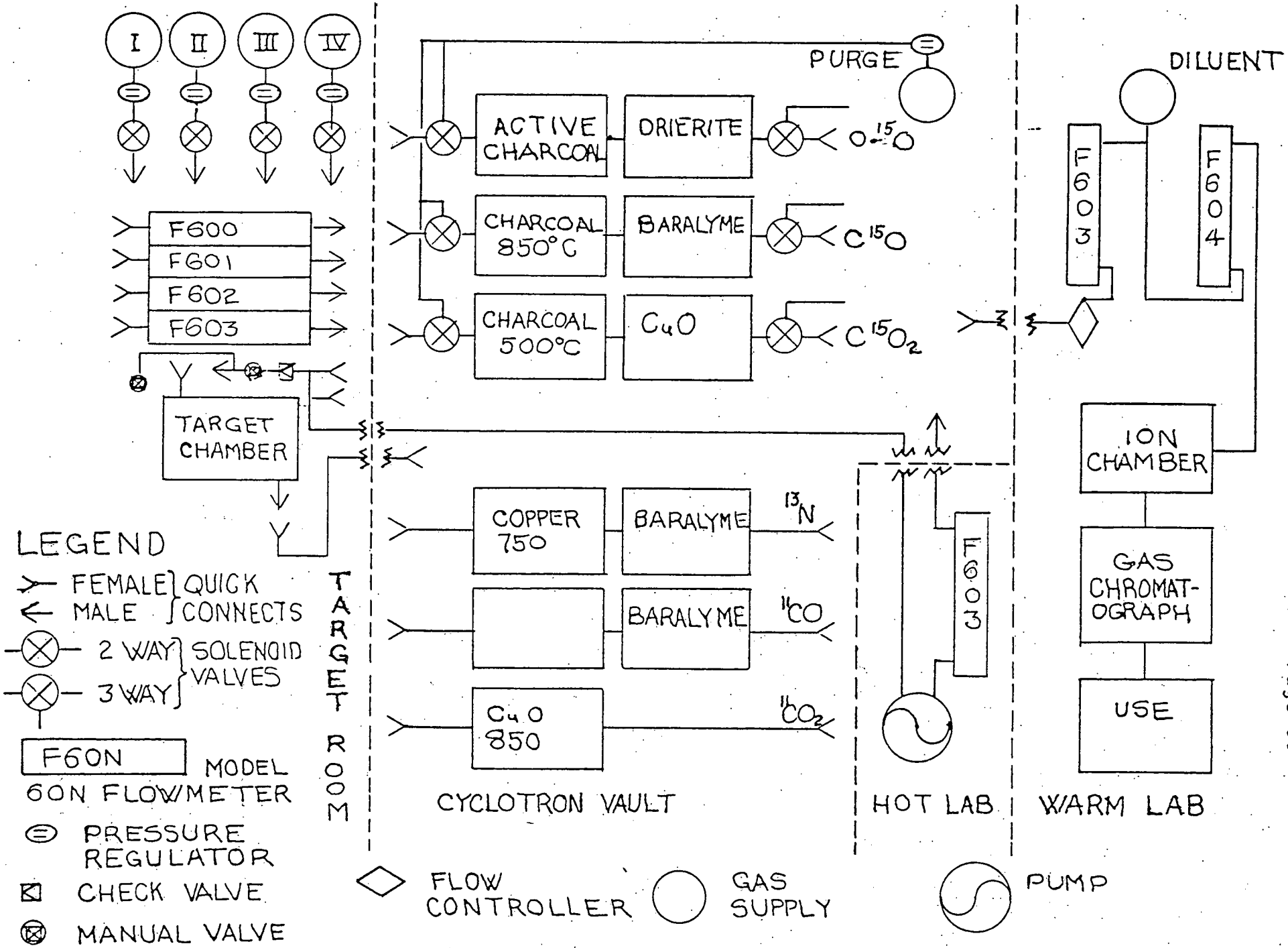

To produce high concentrations of $C^{15}O.O$ in nitrogen, a recirculating pump (Metal Bellows, Inc., Model MB21), flowmeter with metering valve, (Matheson Gas Products, Model 603) and a return line were installed as in Figure 1. The pump and flowmeter are situated in the cave in the hot laboratory. A tap with a Luer connector to accept a standard disposable syringe is in the return line on top of the pump, to allow withdrawal of the product. Valving on the target return line at the target chamber connection permits flushing the system before irradiation to insure proper composition of the target gas. Two different target gases have been tried. Using 1% O_2 in N_2, the yield was 4 mCi $C^{15}O.O$/50 ml N_2 at a beam current of 20 μAmp. Radiochemical purity was 98%. Total CO_2 concentration was 0.6%. The other target gas used was nitrogen with 1 - 2% CO_2 added. Recirculating at 1.75 l/min., 1.8% CO_2 in the target gas gave a yield of 14 mCi $C^{15}O.O$/50 ml gas with a purity greater than 99%. The only contaminant was ^{13}N, about 0.3%. The ^{13}N level is minimized by using a target chamber beam entrance foil of aluminum of 0.3125 g/cm^2 thickness. This reduces the energy of the deuteron beam incident on the target gas to 5.3 MeV, preventing the reaction ^{14}N (d,T) ^{13}N. Nitrogen-13 in the product is detectable by following the half-life of a peak trapped after separation from the sample by gas chromatography on molecular sieve 5A.

REFERENCES

1. Watson, D.D., Kenney, P.J., Gelband, H., Tamer, D.R., Janowitz, W.R., Sankey, R.R., Finn, R.D., Hildner, F.J., & Gilson, A.J. A non-invasive technique for the study of cardic hemodynamics utilizing $C^{15}O_2$ inhalation. Nuclear Medicine. 119:615, 1976.

2. U.S. ERDA Proposal "Biomedical Research and Application Utilizing Cyclotron Produced Radionuclides". Jan 1, 1977 to Dec 31, 1977.

3. Progress Report to U.S. AEC contract at (30-1) 910, NYO 910-150. "Biological Effects of Radation and Related Biochemical and Physical studies". For period May 1, 1969 to May 1, 1970.

4. Progress Report to U.S. ERDA contract #EE-77-5-02-4268-002. "Biomedical Research and Application Utilizing Cyclotron Produced Radionuclides. For period October 1, 1976 to September 1977.

5. Proposal to the National Foundation - The March of Dimes, Study of Cardiac Hemodynamics in Infants and Children with Congenital Heart Disease Utilizing Oxygen Labelled Carbon Dioxide ($C^{15}O$). Submitted by Cornell University Medical College in collaboration with Sloan-Kettering Institute.

2. RADIODRUG RESEARCH AND DEVELOPMENT

2.1. ^{11}C-LABELED COMPOUNDS

2.1.1. ^{11}C-AMINO ACIDS

OBJECTIVE:

To synthesize DL-valine-1-^{11}C, ^{11}C-DL-tryptophan, ^{11}C-1-aminocyclopentane-carboxylic acid, and related compounds in millicurie amounts, and to evaluate these compounds as potential tumor or pancreatic scanning agents.

SCOPE OF INVESTIGATION:

Since pancreatic tissue synthesizes protein it is expected that carbon-11 labeled amino acids would be taken up in the pancreas. Busch et al. (1) have measured the uptake of various carbon-14 labeled amino acids in the pancreas and other tissues and have found that valine has one of the highest pancreatic uptakes. Experiments with transplantable animal tumors have demonstrated that carbon-14 labeled amino acids are incorporated into tumor tissue at a greater rate than into normal tissue (2). The synthesis of valine-^{11}C would provide an agent which has a demonstrated high degree of localization in the pancreas. This localization is almost twice that of ^{75}Se-seleno-methionine the agent currently in use. This should provide improved visualization of the pancreas, leading to detection of smaller lesions, with acceptance of greatly reduced radiation exposures.

Carbon-11 has been made in our laboratory in amounts up to 1.5 Curies by proton irradiation of nitrogen either as methane-^{11}C when hydrogen is added to the target gas, or as carbon dioxide-^{11}C when oxygen is present in the target gas. The methane-^{11}C was converted to hydrogen cyanide-^{11}C by reaction with ammonia on a platinum catalyst at 1000°C, according to the method of Christman et al. (3). We have used the H^{11}CN so produced to synthesize DL-valine-1-^{11}C, as shown below, by a modification of the hydantoin procedure developed by us to produce dilantin (4) and by Hayes, Washburn and co-workers at Oak Ridge to produce ^{11}C-aminocyclopentane carboxylic acid (5,6).

Synthesis of DL-Valine-1-^{11}C

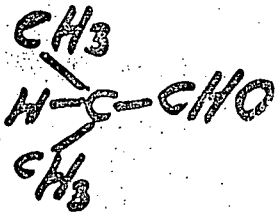

Isobutyraldehyde

$H^{11}CN$ KCN
$(NH_4)_2\ CO_3$

Steel Bomb
210°C
10 min.

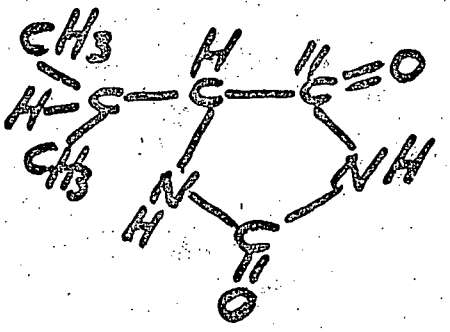

Hydantoin Intermediate

Alkaline Hydrolysis
Steel Bomb
210°C
10 min.

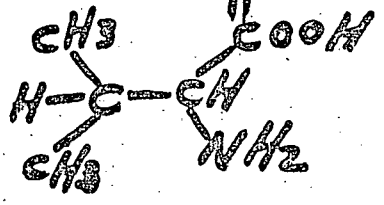

DL-Valine
70% yield-overall

Purification of DL-Valine

1) Anion Exchange
   AG 1-X8
   (hydroxide form)
   100-200 mesh
2) Cation Exchange
   AG 50W-X2
   (hydrogen form)
   50-100 mesh

RESULTS AND CONCLUSIONS:

By this procedure, DL-valine labeled with carbon-11 has been synthesized in twelve separate batches in amounts up to 25 mCi in about one hour.

As shown in this scheme isobutyraldehyde, ammonium carbonate, and carbon-11 labeled cyanide are reacted at high temperature and pressure for a short time to produce the hydantoin of isobutyraldehyde. After cooling, the hydantoin is hydrolyzed under high temperature and pressure to DL-valine in 70% yield. The product was purified by ion exchange chromatography on Bio-Rad AG-1 and AG-50 resins. Assay of the product by thin layer chromatography showed the radiopurity to exceed 95%. In a typical experiment, $H^{11}CN$ is bubbled into a glass gas absorption column containing 3 ml of 0.005 N NaOH. This solution (containing $Na^{11}CN$) is drained through a stopcock at the base of the column into a stainless steel pressure vessel having an internal volume of 20 ml. The reaction vessel is charged with a mixture of 85.7 mg isobutyraldehyde, 216 mg $(NH_4)_2 CO_3$, 20.1 mg NH4CL and 18.6 mg NaCN, prior to introduction of the $H^{11}CN$. The closed vessel is heated rapidly to 210°C and maintained at that temperature for 10 minutes after which it is rapidly cooled. Three ml of 6N NaOH is then introduced and the vessel is again heated at 210°C for another period of 10 minutes. The cooled reaction mixture is filtered and then loaded directly onto a 1.5 cm diameter X 5 cm length prewashed AG 1-X2, 100-200 mesh, anion exchange bed (Bio-Rad, Laboratories, Rockville Centre, New York) in the hydroxide form. Anionic components, including ^{11}C-valine are retained by the column while cationic and non-ionic components pass through. After washing repeatedly with distilled water (∿ 50 ml) the column is then eluted with 1 N HCl, the process being monitored by means of an ion chamber. This eluate (∿ 15 ml) is then loaded onto a prewashed 1.0 cm (diameter) x 15 cm (length) AG 50W-X2, 50-100 mesh, cation exchange bed (Bio-Rad Laboratories) in the hydrogen form. Cationic material (^{11}C-valine) is retained while anionic material passes through the column. After being washed repeatedly with distilled water (∿ 50 ml), the column is slowly eluted with 0.2 N NaOH, the process again being monitored with an ion chamber to minimize the volume of eluate containing the product (∿ 10 ml). The purified ^{11}C-valine solution can then be adjusted to physiologic pH with HCl and sterilized by microfiltration for investigational use. Generally overall chemical yields of about 70% were obtained. The purity of the ^{11}C-valine product was assessed by thin layer chromatography (tlc) using Eastman silica gel chromagram sheets (13179) developed in butanol:water:acetic acid (100:10:5 v/v).

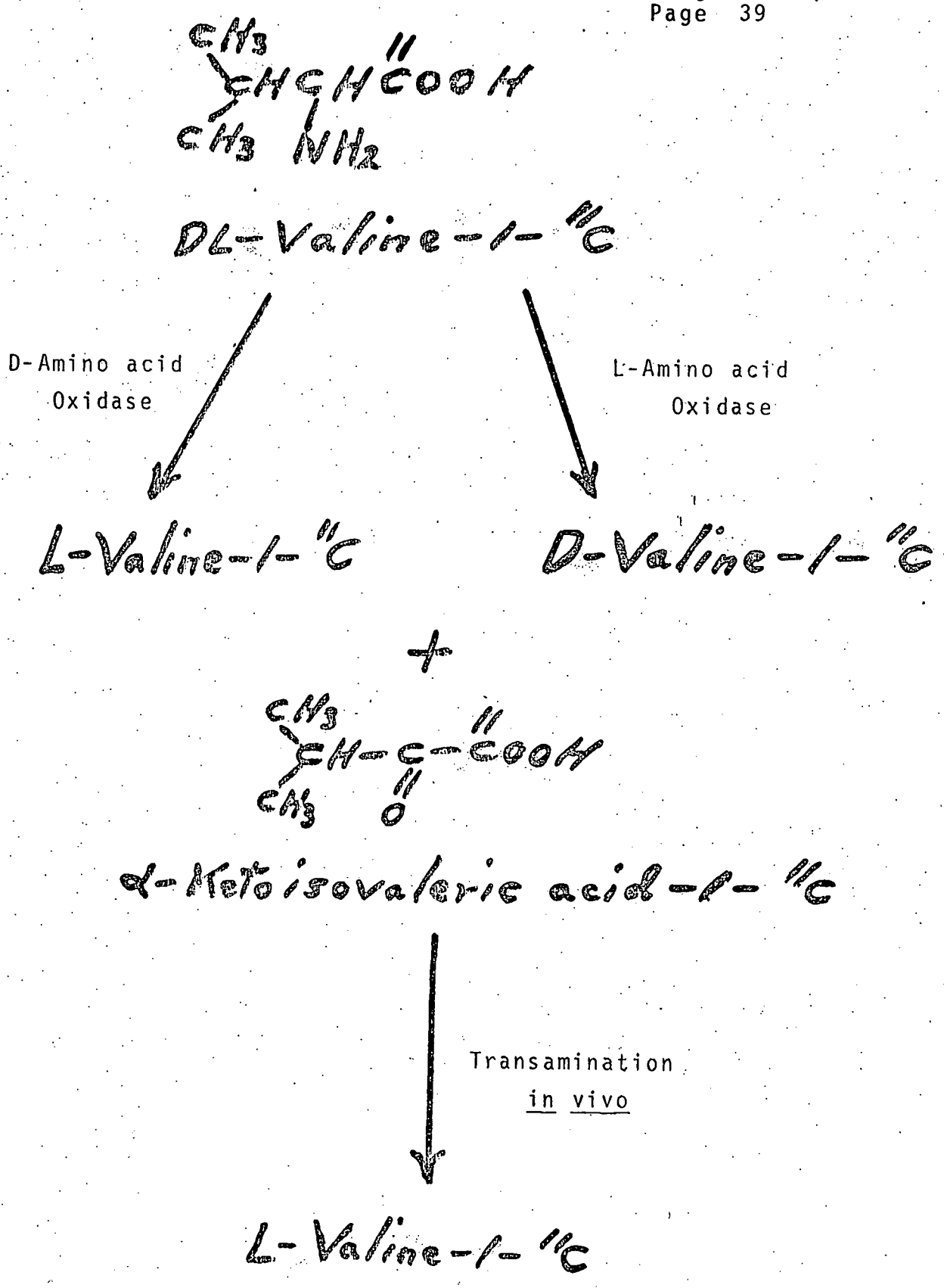
DL-Valine-1-14C
D-Amino acid Oxidase
L-Amino acid Oxidase
L-Valine-1-14C
D-Valine-1-14C
+
α-Keto isovaleric acid-1-14C
Transamination in vivo
L-Valine-1-14C

At present, specific activities of DL-valine-1-^{11}C up to 1 mCi/mg have been obtained. About a three-fold increase in specific activity can be obtained by reducing the amount of unlabeled cyanide used in this reaction. A pressure vessel having an internal volume of 3 ml is required for this purpose, and its construction for our use has now been completed.

DL-valine synthesized by this procedure has been administered to Sprague-Dawley rats and mongrel dogs. A positive uptake in the pancreas was observed in both species. In the rat, the relative concentrations in the pancreas and liver were about 6.0 and 1.5 respectively. In the dog, relative concentrations of 4.0 and 2.0 were obtained. Neither species were conditioned prior to administration of DL-valine. In one experiment with an unconditioned Rhesus monkey, visualization of the pancreas was equivocable.

The utility of DL-valine as a pancreatic scanning agent has been demonstrated in patients by the Oak Ridge investigators (7). Among nine patients studied, six showed the pancreas clearly, two did not show it clearly, and one did not show it at all. In general, these results look promising and we are presently conducting pyrogenicity tests on our preparations of DL-valine and hope to begin clinical studies in the near future.

Since DL-valine appears promising as a pancreatic imaging agent, we thought that L-valine may be an even better imaging agent. In fact, a comparison of uptake in normal Sprague-Dawley rats of L-valine-^{13}N, produced enzymatically in our laboratory with DL-valine-1-^{11}C, produced by chemical synthesis, have shown that L-valine-^{13}N has about 1.6 times the relative concentration in the pancreas, at 20-60 minutes post-injection as does DL-valine-1-^{11}C. We have recently prepared L-valine-1-^{11}C in reactions catalyzed by the specific action of D-amino acid oxidase (8,9) on Dl-valine-1-^{11}C, as shown below. In a similar, manner, D-valine-1-^{11}C was prepared utilizing L-amino acid oxidase. Resolution of DL-valine-1-^{11}C by this method led to the formation of equimolar amounts of α-keto-isovaleric acid-1-^{11}C. Since α-keto acids undergo transamination reactions <u>in vivo</u> to L-amino acids, tissue distribution studies with α-keto-isovaleric acid-1-^{11}C are of interest.

By this procedure, L- and D-valine-1-^{11}C have been synthesized in amounts up to 4 mCi from 16 mCi of DL-valine-1-^{11}C. An equivalent amount (4 mCi) of α-keto-isovaleric acid-1-^{11}C was obtained.

In a typical reaction, DL-valine is buffered to pH 7.8-8.4 with sodium borate and treated at 37° with D-amino acid oxidase in the presence of catalase to produce equimolar amounts of L-valine and α-ketoisovaleric acid. These products are separated by ion exchange chromatography on an AG-1-X8 anion

exchange resin (acetate form). The enzymatic reaction mixture is added directly to the column and the column is eluted with water to yield L-valine. After the amino acid is removed, the α-keto acid remaining on the column is eluted with IN KCL.

At this time, only two experiments have been performed and we are presently working out the details of the enzymatic reaction and purification of the products.

In addition to synthesizing L-valine-1-^{11}C, we are also interested in preparing ^{11}C labeled L-tryptophan as a possible pancreatic scanning agent, since tryptophan has a higher degree of localization in the pancreas than valine (1,10). We plan to synthesize (^{11}C-carboxy)-DL-tryptophan by the hydantoin method (11) and to obtain (^{11}C-carboxy)-L-tryptophan from it by enzymatic resolution utilizing D-amino acid oxidase. We are presently working out the details of the process with unlabeled substrates.

Because of the apparent potential of ^{11}C-labeled 1-aminocyclopentanecarboxylic acid (ACPC) as a tumor-scanning agent (5,12) we are interested in synthesizing this and related compounds for evaluation at this Center, and have recently initiated work with unlabeled substrates.

REFERENCES:

1. Busch, H. et al. Amino acid uptake in nuclear proteins. Cancer Res. 19:1030, 1959.

2. Quastel, J.H. and Bickis, I.J. Metabolism of normal tissues and neoplasms in vitro. Nature 183:281-286, 1959.

3. Christman, D.R., Finn, R.D., Karlstrom, K.I., and Wolf, A.P. The production of ^{11}C-HCN---. Int. J. Appl. Rad. Isotopes 26:435-442, 1975.

4. Tilbury, R.S., Stavchansky, S., Ting, C.T., McDonald, J.M., Maugham, E.Z., Freed, B.R., Russ, G.A., Helson, L., Benua, R.S., Kostenbauder, H.B., and Laughlin, J.S. The preparation and evaluation of diphenylhydantoin-C-11 as a tumor scanning agent. J. Nucl. Med. 16:575, 1975. (Abstract)

5. Hayes, R.L., Washburn, L.C., Wieland, B.W., Sun, T.T., Turtle, R.R., and Butler, T.A. Carboxyl-labeled ^{11}C-1-amino-cyclopentanecarboxylic acid, a potential agent for cancer detection. J. Nucl. Med. 17:748-751, 1976.

6. Washburn, L.C., Wieland, B.W., Sun, T.T., Hayes, R.L., and Butler, T.A. (1-^{11}C) DL-valine, a potential pancreas-imaging agent. J. Nucl. Med. 19:77-83, 1978.

7. Andrews, G.A., Hubner, K.F., Washburn, L.C., Wieland, B.W., Gibbs, W.D., Hayes, R.L., and Butler, T.A. Clinical studies of C-11-labeled amino acids. J. Nucl. Med. 18:638, 1977. (Abstract)

8. Cooper, A.J.L., Stephani, R.A., and Meister, A. Enzymatic reactions of methionine sulfoximine. J. Biol. Chem. 251:6674-6682, 1976.

9. Worthington Enzyme Manual, ed. L. A. Decker. Worthington Biochem. Corp., Freehold, New Jersey 07728, 1977, p. 51.

10. Washburn, L.C., Sun, T.T., Wieland, B.W. and Hayes, R.L. C-11-DL-Tryptophan, a potential pancreas imaging agent for positron tomography. J. Nucl. Med. 18:638, 1977. (Abstract)

11. Hayes, R.L., Washburn, L.C., Wieland, B.W., Sun, T.T., Anon, J.B., Butler, T.A., and Callahan, A.P. Synthesis and purification of ^{11}C-carboxyl-labeled amino acids. Int. J. Appl. Radiat. Isotopes 29:186-187, 1978.

12. Hubner, K.F., Andrews, G.A., Washburn, L.C., Wieland, B.W., Gibbs, W.D., Hayes, R.L., Butler, T.A., and Winebrenner, J.D. Tumor location with 1-aminocyclopentane-(^{11}C)-carboxylic acid: Preliminary clinical trials with single-photon detection. J. Nucl. Med. 18:1215-1221, 1977.

2.1.2. PREPARATION OF ^{11}C-LABELED PRECURSORS

OBJECTIVE:

The object of this work is the development of apparatus and procedures to routinely, reliably, and easily produce simple ^{11}C labeled compounds (e.g. ^{11}CN, H ^{11}CHO, $^{11}CH_3I$) for use in preparing ^{11}C labeled materials of clinical interest.

SCOPE OF INVESTIGATION:

Carbon-11 has previously been produced at this laboratory as H ^{11}CN by the proton bombardment of nitrogen containing up to 5% added hydrogen (1). Similar to methods used in some other laboratories (2,3), this method requires the formation of $^{11}CH_4$ in the target. It has been reported that $^{11}CH_4$ is the primary ^{11}C species produced at high dose rates and is not retained in the target (2). Experience in this laboratory has shown that efficient removal of ^{11}C from the target requires a beam of at least 35 μAmp and must be focused to pass through a 1 cm collimator. The need to finely focus beams of 35 μAmp minimum requires very careful cyclotron maintenance and tuning, beyond the normal and easily achievable routine.

The production of compounds other than H ^{11}CN is simpler then CO_2 is the starting material. Carbon-11 CO_2 is easily produced by the proton bombardment of nitrogen containing one to five percent oxygen. No difficulties are encountered with recovery of the activity and the composition of the product should be independent of the radiation dose, at least within the ranges of this work. The conversion of $^{11}CO_2$ to other materials such as H ^{11}CHO, and $^{11}CH_3I$, is well documented (4,5). The synthesis of ^{11}C-labeled compounds of clinical interest requires many different simple ^{11}C precursors. The precursor compounds must be readily available to the synthetic organic radiochemist. The requirement is for a system of targetry and processing apparatus sufficiently simple to operate and sufficiently integrated with the cyclotron to permit the synthetic chemist to regard the assemblage as a carbon-11 precursor dispensing machine.

RESULTS AND CONCLUSIONS:

Figure 3 is a diagram of the system used at Sloan-Kettering Institute for producing simple compounds labeled with ^{11}C which in turn provide a means of preparing more complex ^{11}C labeled compounds, such as ^{11}C-valine or ^{11}C-dilantin. One per cent oxygen in nitrogen is used as target gas supplied, pre-mixed, from a pressure tank through a two stage pressure reducing regulator, remotely controlled solenoid valve, and flowmeter to

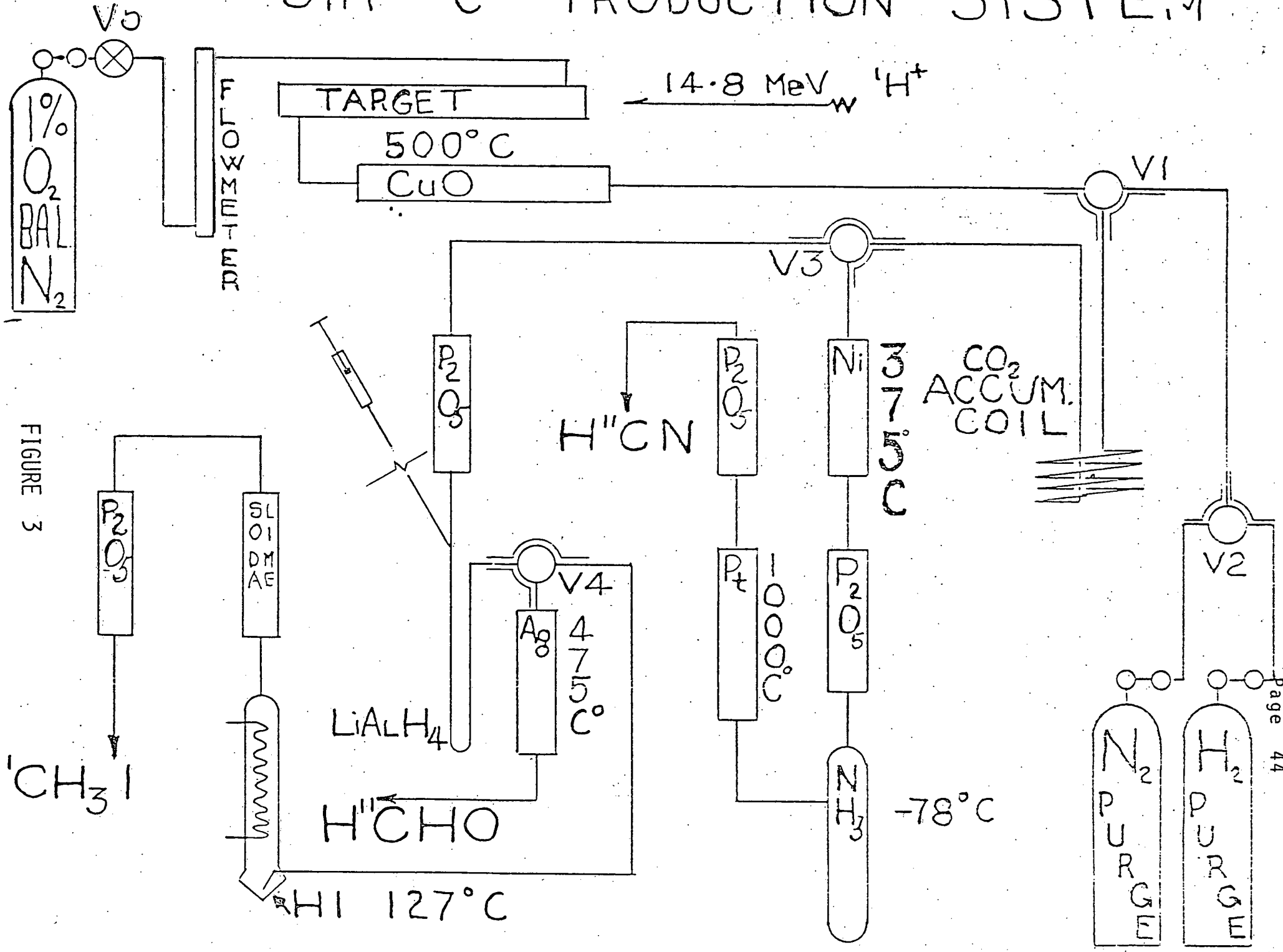
SKI "C PRODUCTION SYSTEM
V5
1% O2 BAL N2
FLOWMETER
TARGET
500°C
CuO
14.8 MeV H+
V1
V3
P2O5
H"CN
P2O5
Ni
375°C
CO2 ACCUM. COIL
V2
P2O5
SLIDMAE
V4
Ag
475°C
LiALH4
Pt
1000°C
P2O5
H"CHO
NH3
-78°C
'CH3I
HI 127°C
N2 PURGE
H2 PURGE
FIGURE 3
Progress Report
Page 44

the flow-through target. A beam of 14.8 MeV protons is degraded to 14.0 MeV by the necessary beam exit foil, target entry foil, and air cooling, before it enters the target gas. The 60 cm target length was selected to stop all the incident proton beam at 3.5 Kg/cm^2 target gas pressure. Carbon-11 produced by the (p,α) reaction of ^{14}N reacts with the oxygen in the target gas and then passes over copper oxide at 500°C to be collected as $^{11}CO_2$ in the nickel accumulator coil. The process system is designed to allow the production of $H^{11}CN$, $^{11}CH_3I$, and $H^{11}CHO$ as required simply by the remote operation of a few valves. Although ^{11}C is produced and collected with a flowing system, the conversion to one or another compound is a batch operation. At the entrance to the processing apparatus a 3-way solenoid valve, V1 allows either irradiated gas from the target or a purge gas to be passed through a 2 mm/D stainless steel coil cooled by liquid nitrogen in a remotely moved Dewar flask. $^{11}CO_2$ in the target gas is condensed in the coil. Oxygen and nitrogen condense in the accumulator coil as a liquid and are blown to warm parts of the coil by the gas flow, to be revaporized. $^{11}CO_2$ will trap as a solid and remain immobile. Solenoid valve V2 allows the selection of nitrogen or hydrogen as purge gas, depending on the product desired. To make $H^{11}CN$, after sufficient activity has been collected in the coil, the target gas flow is stopped and the coil purged with hydrogen for two minutes, passing the off gas to waste. Following a two minute purge, the gas is then directed through the $H^{11}CN$ apparatus by solenoid valve V3. The Dewar containing liquid nitrogen cooling the accumulator coil is lowered. As the temperature of the trap increases the $^{11}CO_2$ is released into the hydrogen stream, swept through the Raney nickel controlled at 375°C where conversion to $^{11}CH_4$ occurs. After drying by passage over P_2O_5, the gas is passed over liquid NH_3 at -78°C to pick up a trace of ammonia. The mixture of $^{11}CH_4$, NH_3 and hydrogen passes over Pt wool at 1000°C where conversion to $H^{11}CN$ takes place. After passage over P_2O_5, the $H^{11}CN$ is collected in the solvent required by the next synthesis.

Methanol labeled with ^{11}C, required to make both $^{11}CH_3I$ and $H^{11}CHO$ is prepared by collecting $^{11}CO_2$ until sufficient activity is accumulated, then purging for two minutes with nitrogen. When the $^{11}CO_2$ is released by lowering the Dewar with the liquid nitrogen, using V3 to direct the gas flow through the lithium aluminum hydride bubbler allows formation of the methanol salt in the lithium aluminum hydride. The $LiAlH_4$ is generally dissolved in tetrahydroforan and an ice bath used to minimize solvent loss. After all $^{11}CO_2$ is reacted, the ice bath is removed and the tetrahydroforan allowed to evaporate. Water is injected into the bubbler containing the lithium salt and the ^{11}C-methanol distilled by means of a hot air gun. Passage of the ^{11}C-methanol over silver wool at 475°C converts it to $H^{11}CHO$.

$^{11}CH_3I$ will be made by passing the $^{11}CH_3OH$ through refluxing HI. At 40 μAmps of protons, 600-700 mCi:$H^{11}CN$ are produced about 5 minutes after taget gas flow is halted. Target

gas is flowed about 1/2 hour. Nine millicuries of $H^{11}CHO$ was prepared 25 minutes after $^{11}CO_2$ collection was halted. A 10 μAmp beam was used in this case.

Continued development of this system will include devising a more efficient $LiAlH_4$ bubbler, a system to remotely monitor the course of the activity as it passes through the system, and improved remote control.

Plans, specifications and a list of equipment and supplies used in this work have been given to Dr. David Elmaleh of Massachusetts General Hospital to assist them in construction of a similar system there.

REFERENCES:

1. Progress Report, U.S. A.E.C. Contract #AT(11-1)-3521, Biological Effects of Radiation and Related Biochemical and Physical Studies, Proposal No. 1. May 1, 1973 to October 31, 1974.

2. Christman, D.R., Finn, R.D., Karlstrom, K.I., and Wolf, A.P. The production of ultra high activity ^{11}C-labeled hydrogen cyamide, carbon dioxide, carbon monoxide, and methane via the ^{14}N (p,α) ^{11}C reaction (XV). Int. J. Appl. Rad. Isotopes 26:435-442, 1975.

3. Lamb, J.F., James, R.W. and Winchell, H.S. Recoil synthesis of high specific activity ^{11}C-cyanide. Int. J. Appl. Rad. Isotopes 22:475-479, 1971.

4. Marazano, C., Maziere, M., Berger, G., and Comar, D. Synthesis of methyl iodide-C and formaldehyde-^{11}C. Int. J. Appl. Rad. Isotopes 28:49-52, 1977.

5. Palmer, A.S. The preparation of ^{11}C-methyl labeled 1,1'-dimethyl 1-4,4' dypridinium dilodide. J. Labeled Compounds Radiopharm. XIV; 1:27-33, 1977.

2.2. ^{13}N LABELED COMPOUNDS

OBJECTIVE:

To synthesize ^{13}N-labeled compounds that will be used in metabolic studies and as tumor and/or organ scanning agents.

SCOPE OF INVESTIGATION:

The enzymatic synthesis of ^{13}N amino acids yields a product with the following attributes:

1. The amino acid is synthesized as the biologically active L-isomer.

2. The amino acid is labeled with ^{13}N, an isotope of a natural constituent of the compound.

3. ^{13}N is a positron emitter which is useful for scanning by positron emission tomography.

RESULTS:

Much of our effort during the past year has been directed toward making ^{13}N-glutamate suitable for patient studies. The glutamate dehydrogenase was immobilized on an activated Sepharose column and ten consecutive mock preparations of labeled glutamate prior to patient studies proved to be free of pyrogens. Clinical studies were begun in April, 1978 and the results will be discussed elsewhere in the report. A total of 27 studies have been carried out in this six month period with as much as five cases per week. With the exception of a two week period when there was some difficulty with the ammonia delivery system, 40-80 mCi of ^{13}N-glutamate were routinely synthesized which was several times more than necessary for the clinical trials. No undesirable side effects have been observed in patients or volunteers. Although the immobilized columns are enzymatically active for months, the labeled product may contain pyrogens when synthesized from a column that has been used for several weeks. We routinely prepare a new column every second week. Limulus tests are carried out on all samples and selected batches are sent out for rabbit pyrogen tests.

Our studies with other ^{13}N-amino acids and ^{13}N-ammonia have continued but at a lower level of priority. ^{13}N-ammonia is produced for the hepatic encephalopathy studies in collaboration with the Neurology Department of Cornell University Medical College. ^{13}N-L-glutamic acid and ^{13}N-L-valine have been prepared

for studies comparing organ distribution in rats with these amino acids labeled uniformly or in the carboxyl position with carbon-14. ^{13}N-L-glutamic acid, L-glutamine and ^{13}N-ammonia are being tested as tumor imaging agents in spontaneous canine tumors in cases supplied by the Animal Medical Center.

We have continued our studies on the synthesis of ^{13}N-L-aspartic acid, L-tyrosine and L-phenylalanine by transaminating oxalacetic acid, hydroxyphenylpyruvic acid and phenyl pyruvic acid respectively with ^{13}N-L-glutamic acid. The reactions are catalyzed by commercial preparations of glutamate-oxolacetate transaminase (GOT) purified from pig heart. The failure of GOT preparations obtained from different commercial laboratories to catalyze the transamination of the α-keto acids of the aromatic amino acids suggests that tyrosine amino transferase is an impurity in some commercial preparations of GOT. The α-keto acids of methionine and dihydroxyphenylalanine but not valine, asparagine or tryptophan can be transaminated by the enzyme preparations. The products were identified by separation on a Partisal SAX column using high pressure liquid chromatography.

CONCLUSIONS:

40-80 mCi of ^{13}N-glutamic acid are synthesized on a routine schedule for clinical evaluation as a tumor and/or organ (pancreas, heart) imaging agent. The glutamate dehydrogenase is immobilized on an activated Sepharose support. The product is sterile, apyrogenic and is suitable for patient injection within ten minutes EOB. Studies on the synthesis of ^{13}N-L-tyrosine, ^{13}N-L-phenylalanine, ^{13}N-L-aspartic acid, ^{13}N-L-methionine and ^{13}N-L-dehydroxy phenylalanine by transaminating ^{13}N-L-glutamate continue.

2.3. ^{18}F-LABELED COMPOUNDS

2.3.1. ^{18}F-4-FLUOROESTRADIOL

OBJECTIVE:

To prepare 4-fluoroestradiol labeled with fluorine-18.

SCOPE OF INVESTIGATION:

About 40% of breast tumors are hormone dependent, and an *in vitro* test has been developed in this Institute to measure the estrogen receptivity of biopsy samples and to use this as a diagnostic aid in the management of patients with breast cancer (1). Estrogen receptive tumor tissue takes up tritiated estradiol *in vitro* about ten times more than normal breast tissue. Experiments at the estrogen receptor protein laboratory in Memorial Hospital, as reported in a previous progress report, have shown 4-F-estradiol to have comparable physiological activity to estradiol itself. If we are successful in labeling estradiol with ^{18}F in the four-position, this compound can be evaluated as a scanning agent for breast cancer or metastases which are hormone dependent. Since estrone is in reversible equilibrium with estradiol, 4-fluoroestrone will be synthesized also.

The synthesis of non-radioactive 4-fluoroestradiol and 4-fluoroestrone has been reported by Utne (2). A modification of Utne's method to the synthesis of these estrogens labeled with ^{18}F has been made in this laboratory.

^{18}F-fluoroestrone and ^{18}F-4-fluoroestradiol can be made by the following scheme utilizing an adaptation of the Schiemann reaction for the introduction of fluorine into an aromatic ring (3,4).

RESULTS AND CONCLUSIONS:

Estrone was used as a starting material rather than estradiol because the diazotization reaction on 4-aminoestradiol-3-methyl ether gave no solid fluoroborate salt but dark oils only (2). Attempts will be made to use estradiol as a starting material by protection of the 17-hydroxy group prior to diazotization.

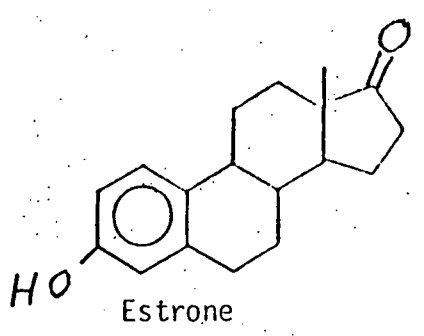

Estrone

Nitration

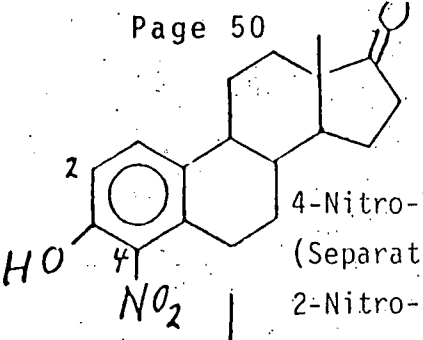

4-Nitro-Estrone
(Separate from
2-Nitro-Estrone

Methylation

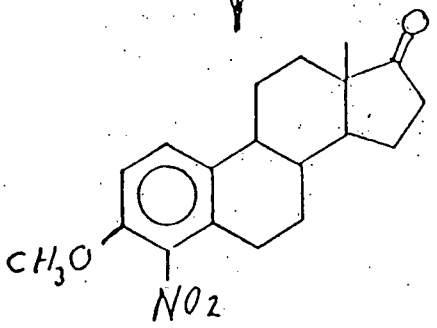

Reduction

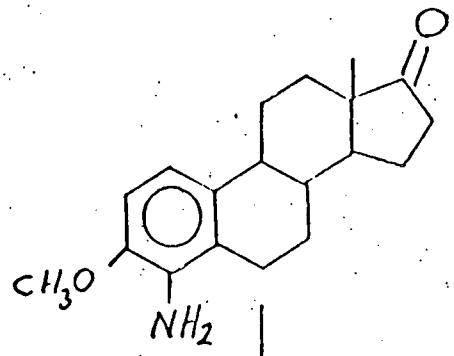

Diazotization

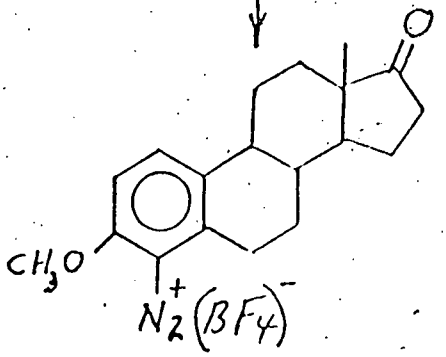

$^{18}F^-$ Exchange

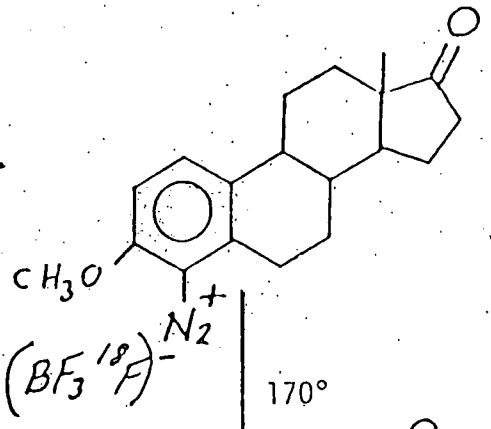

170°

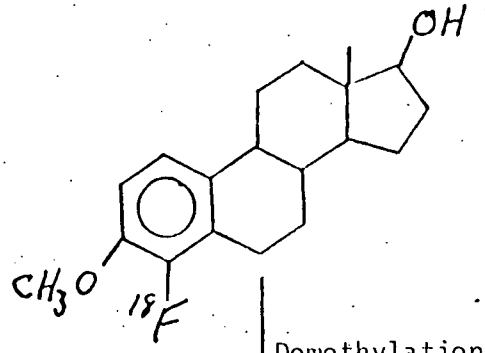

Reduction

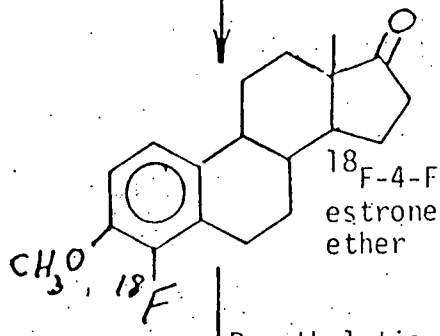

^{18}F-4-Fluoro-
estrone methyl
ether

Demethylation

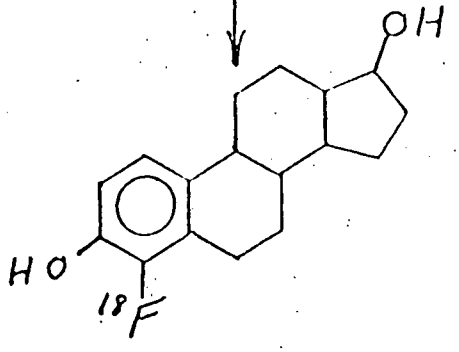

^{18}F-4-Fluoroestradiol

Demethylation

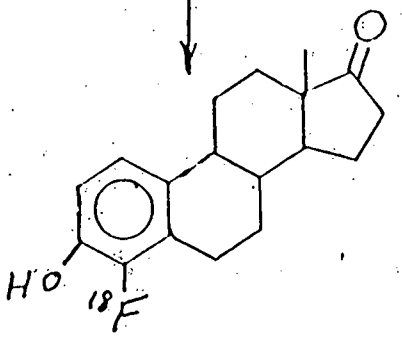

^{18}F-4-Fluoroestrone

The procedure described below permits the production of ^{18}F-4-fluoroestradiol in amounts up to 500 μCi in about 5 hours with specific activities of $\frac{300\ \mu Ci}{mg}$. Although, several batches of ^{18}F-4-fluoroestrone-methyl ether have been prepared, only one preparation of ^{18}F-4-fluoroestradiol has been made at this writing. This preparation was used in an experiment in a mouse in which ^{18}F-4-fluoroestradiol and tritiated estradiol were simultaneously evaluated. Although we have the data for this study, we wish to confirm these results with at least one more study before reporting them as reproducible.

^{18}F$^-$ was produced by cyclotron through the ^{16}O(^{3}He,P) ^{18}F reaction and up to 500 μCi of ^{18}F$^-$ in 20 ml of water was obtained. The volume of the water was reduced to about 1 ml by heating in a large conical tube in an oil bath for 20-30 minutes.

After cooling, 20 mg of the diazonium tetrafluoroborate salt of the methyl ether of estrone in 2 ml acetonitrile was added to the ^{18}F$^-$ solution. The reaction mixture was allowed to stand for 5 minutes to enhance the incorporation of ^{18}F into the tetrafluoroborate moiety. The solvents were evaporated to dryness at 30° under high vacuum in a preheated aluminum block for about 30 minutes. At this writing, the pyrolysis time has not been optimized. We are presently working out the details of this step. After cooling, chloroform was added to dissolve the amber pyrolysate. The solution was heated to boiling in a preheated aluminum block to completely extract the product from any resinous material adhering to the wall of the tube. The chloroform solution was concentrated at 50° to a small volume and added directly to a column of alumina (benzene). The product, ^{18}F-4-fluoroestrone methyl ether, was eluted from the column with 20 ml of chloroform and the eluant was evaporated to dryness at 50° under nitrogen. The residue in 0.8 ml of tetrahydrofuran was chilled to 0-5° and treated with a solution of 15 mg of sodium borohydride in a mixture of cold THF (0.2 ml) and methyl alcohol (0.2 ml) at 0-5° for 30 minutes. The solution was acidified by the cautious addition of 0.1 ml of cold 4N hydrochloric acid. Water (0.5 ml) was added and the mixture was stirred at 0-5° for 20 minutes. The solvents were evaporated to dryness on a rotatory evaporator and the dried residue was extracted with chloroform. The chloroform solution was placed in a glass vial and the solvent was evaporated under nitrogen. The residue, containing ^{18}F-4-fluoroestradiol methyl ether, was mixed with 865 mg of pyridine hydrochloride and heated in an aluminum block under pressure (5 ml microflex vial sealed with a microflex valve) at 220° for about 30 minutes (the optimum condition for this step as well as alternative methods of demethylation are presently under investigation). After cooling, the residue was treated with 0.1 N hydrochloric acid and extracted with ether, and the combined extracts were washed with 0.1 N hydrochloric acid and water. The ether layer was extracted

three times with 3 ml portions of 1N potassium hydroxide. The combined alkaline extracts were washed with ether and acidified with concentrated hydrochloric acid, and the organic material was extracted with chloroform. The combined extracts were washed to neutrality with water and the chloroform solution was dried, concentrated to a small volume under nitrogen, and added directly to a column of alumina (benzene). The product, ^{18}F-4-fluoroestradiol, was eluted from the column with chloroform. The eluant was evaporated to dryness under nitrogen, and the dried residue was dissolved in 0.5 ml of propylene glycol, ethanol, saline (4:1:5) and sterilized by microfiltration for investigational use. Since the overall chemical yield for the formation of 4-fluoroestradiol from the diazonium salt is about 12% by Utne's procedure (2), the amount of product which can be obtained from 20 mg of the diazonium salt is about 1.7 mg.

The identity of the product was determined by mass spectrometry and by comparison with an authentic sample of unlabeled 4-fluoroestradiol in thin-layer chromatographic analyses. Analytical TLC (silica gel-chloroform/benzene 50:50) showed the product to have a radiopurity greater than 95%. However, the product was not pure, chemically. Estrone and estradiol have been detected by TLC among the products of this synthesis in addition to the fluoro derivatives. Presumably they are derived from reductive decomposition of the diazonium salt. Utne et al. reported analogous results with the 2-fluoro isomer (2). Recently, Palmer et al. (6) prepared ^{18}F-labeled 4-fluoroestrone and 4-fluoroestradiol with specific activities of 100-500 $\frac{\mu Ci}{mg}$ by an adaptation of Utne's procedure. These workers reported that the chemical purity of their products was questionable. We are presently attempting to purify our products by high pressure liquid chromatography.

REFERENCES

1. Nisselbaum, J.S., et al. Estrogen receptors in human breast tissue. 65th Annual Mtg. American Association for Cancer Research, March 27-30, 1974, Houston, Texas. (Abstract)

2. Utne, T., Jolson, R.B. and Babson, R.D. The synthesis of 2- and 4-fluoroestradiol. J. Org. Chem. 33:2469-73, 1968.

3. Firman, G., Nahinias, C., and Garnett, S. The preparation of ^{18}F-5-fluoro-dopa with reactor-produced fluorine-18. Int. J. Appl. Radiation Isotopes 24:182, 1973.

4. Kook, C.S., Reed, M.F. and Digenis, G.A. Preparation of ^{18}F-haloperidol. J. Med. Chem. 18:533, 1975.

5. AMA Drug Evaluations, 3rd edition. Publishing Sciences Group, Inc., Littleton, Massachusetts, 1977, p. 560.

6. Palmer, A.J. and Widdowson, D.A. The preparation of ^{18}F-labeled 4-fluoroestrone and 4-fluoroestradiol. Second International Symposium on Radiopharmaceutical Chemistry, Oxford, England, pp. 14-16, July 1978.

2.3.2. ^{18}F-HALOPERIDOL

OBJECTIVE:

To prepare haloperidol labeled with fluorine-18. Haloperidol is an antipsychotic drug and is of interest to study relative to dilantin as a brain scanning agent. More important perhaps is the possibility of using this labeled compound as an indicator in mental illness.

SCOPE OF INVESTIGATION:

The chemistry (1) pharmacology (2), distribution, excretion, and metabolism in rats (3), of the drug haloperidol have been studied. The interest of our collaborators at the University of Kentucky in obtaining data on tissue distribution and pharmaco-kinetics of the neuroleptic drug haloperidol by external scintigraphic techniques has led them to devise a synthetic route, as described below, for its rapid preparation in the ^{18}F-isotopically labeled form. According to this sequence, the incorporation of ^{18}F into the molecule occurs at the last step through a Schiemann-type reaction which involves the pyrolysis of the diazonium tetrafluoroborate salt (4,5).

The production of haloperidol was favored when the pyrolysis of salt was conducted at 140° for 4 min in a xylene-dioxane (3:1) mixture. In contrast, however, attempts to run the pyrolysis for longer periods of time (30 min), favored production of the olefin 4-[4-(p-chlorophenyl)-2,5,6-trihydroxy-pyridino-4'-fluorobutyrophenone]. The described procedure permits the preparation of (^{18}F)-haloperidol in 120 min with specific activities up to 105 μCi/mg.

It is desirable to produce (^{18}F)-haloperidol with a greater specific activity. In a typical experiment, as described by Kook and co-workers (4,5), the diazonium tetra-fluoroborate salt 2 was not purified. Compound 2 was presumed to be the diazonium fluoroborate salt by its subsequent conversion to haloperidol. By a modification of Kook's procedure, we purified the diazonium fluoroborate salt by dissolving it in acetonitrile and precipitating it with ether. A yellow solid was obtained, m.p. 105°-145° (dec), which can be stored at room temperature for several days without decomposition. This material was presumed to be the diazonium fluoroborate salt by its subsequent conversion to haloperidol.

Under the reaction conditions of Kook et al (4,5), haloperidol and olefin are produced from 2 in yields of 38% and 11% respectively (Figure 4). Olefin is formed from haloperidol by dehydration. Since decomposition of the diazonium fluoroborate salt occurs below 145°, conversion of 2 to haloperidol can be effected at lower temperatures with a concomittant decrease in olefin formation. Consequently, at lower temperature, an increase in specific activity of haloperidol up to 30% might be possible.

A more significant increase in specific activity of haloperidol can be achieved by increasing the radiochemical yield of haloperidol. Tilbury and co-workers (6) have produced ^{18}F by the ^{3}He-irradiation of water at 25 μA for 30 min. Beam currents as high as 50 μA were used successfully with the target system used by these workers. The average yield was 6 mCi/μA for a 1 hr irradiation and the maximum that has been produced in an irradiation of 2 hrs was 500 mCi. Starting with 115 mCi, at end of bombardment, Kook (5) obtained (^{18}F) haloperidol with a total activity of 472 μCi. Since 4.5 mg of haloperidol was prepared from 15 mg of diazonium fluoroborate salt, the specific activity of (^{18}F) haloperidol obtained was 105 μCi/mg. Starting with 500 mCi, at the end of bombardment a 4-fold increase in specific activity of haloperidol should be possible.

RESULTS AND CONCLUSIONS:

By these and other modifications (see section 2.3.1 on ^{18}F-4-fluoroestradiol) we have been able to increase the radiochemical yield of $^{18}F^-$ and to reduce the amount of diazonium fluoroborate salt required for labeling. In four separate batches, ^{18}F-haloperidol was produced in amounts up to 800 μCi with specific activities of 800 μCi/mg in about 120 minutes.

In one experiment in a dog, 100 μCi was administered intravenously and the dogs scanned with the gamma camera (Figure 5). Uptake of ^{18}F-haloperidol in the brain was rapid and reached maximum levels in about 30 minutes after IV administration of the drug, as shown in Figure 6. The drug was found to be slowly eliminated from the brain which seems to correlate well with the prolonged duration of neuroleptic activity of haloperidol.

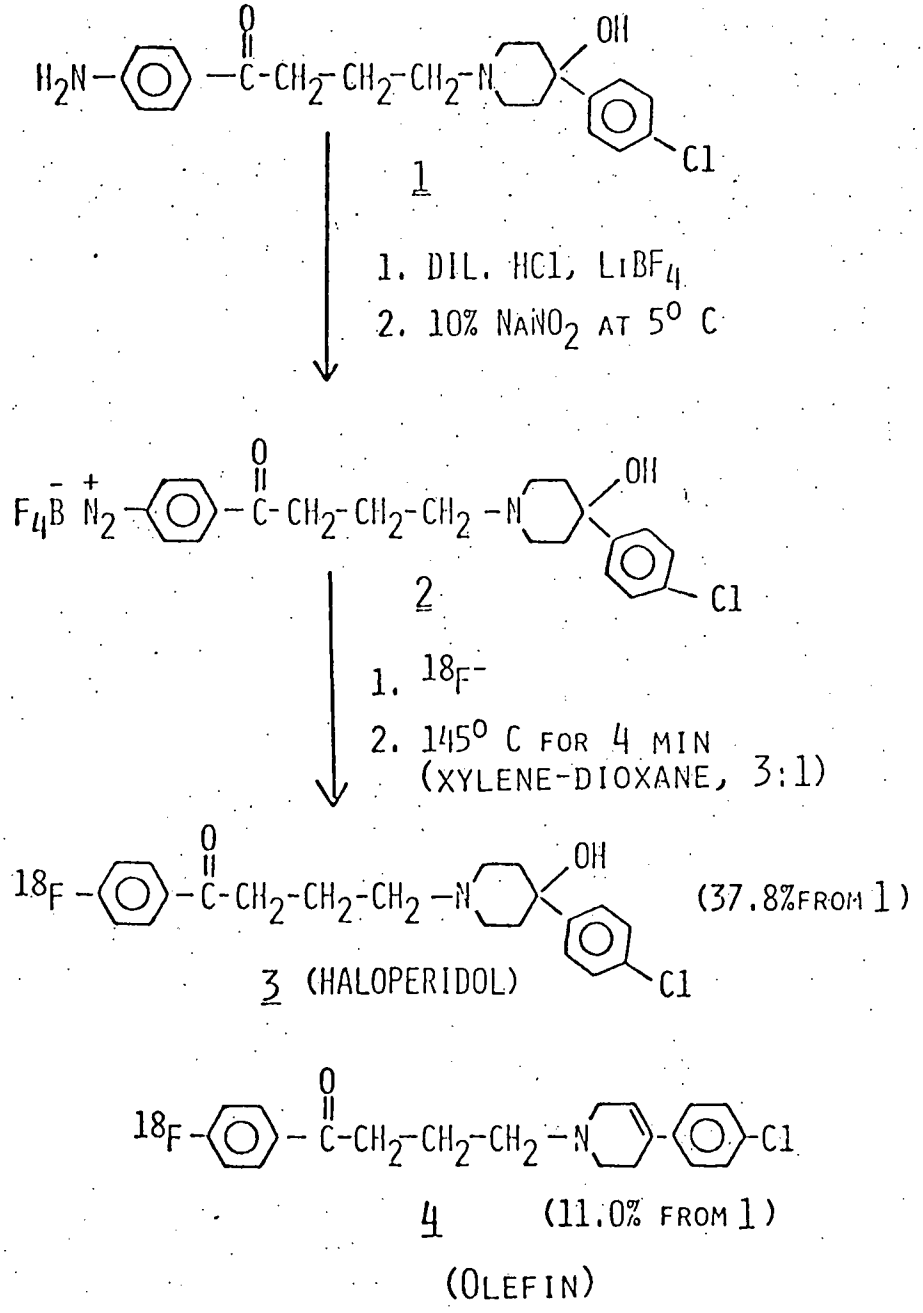
1
1. DIL. HCl, $LiBF_4$
2. 10% $NaNO_2$ AT 5° C
2
1. $^{18}F^-$
2. 145° C FOR 4 MIN
(XYLENE-DIOXANE, 3:1)
(37.8% FROM 1)
3 (HALOPERIDOL)
4
(11.0% FROM 1)
(OLEFIN)

FIGURE 4

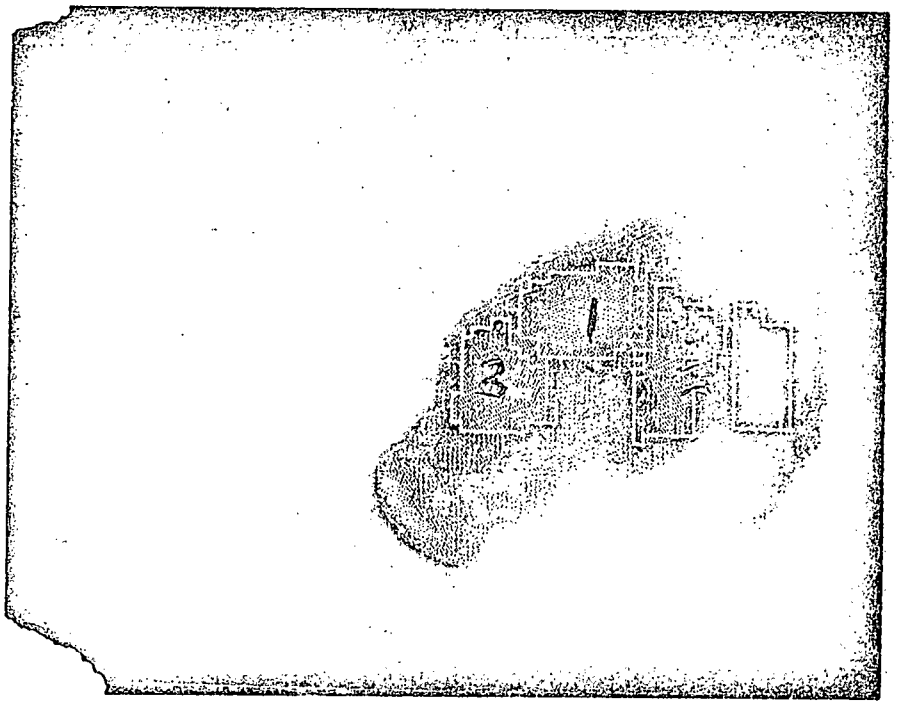

REGION 1 + BRAIN

REGION 2 × POSTERIOR TO BRAIN

REGION 3 ▷ ANTERIOR TO BRAIN

REGION 4 ▽ NECK

FIGURE 5

Tokim dot display, 3 hours following IV injection of ^{18}F-haloperidol (4 μCi/kg). Laterial view of head of dog.

FIGURE 6

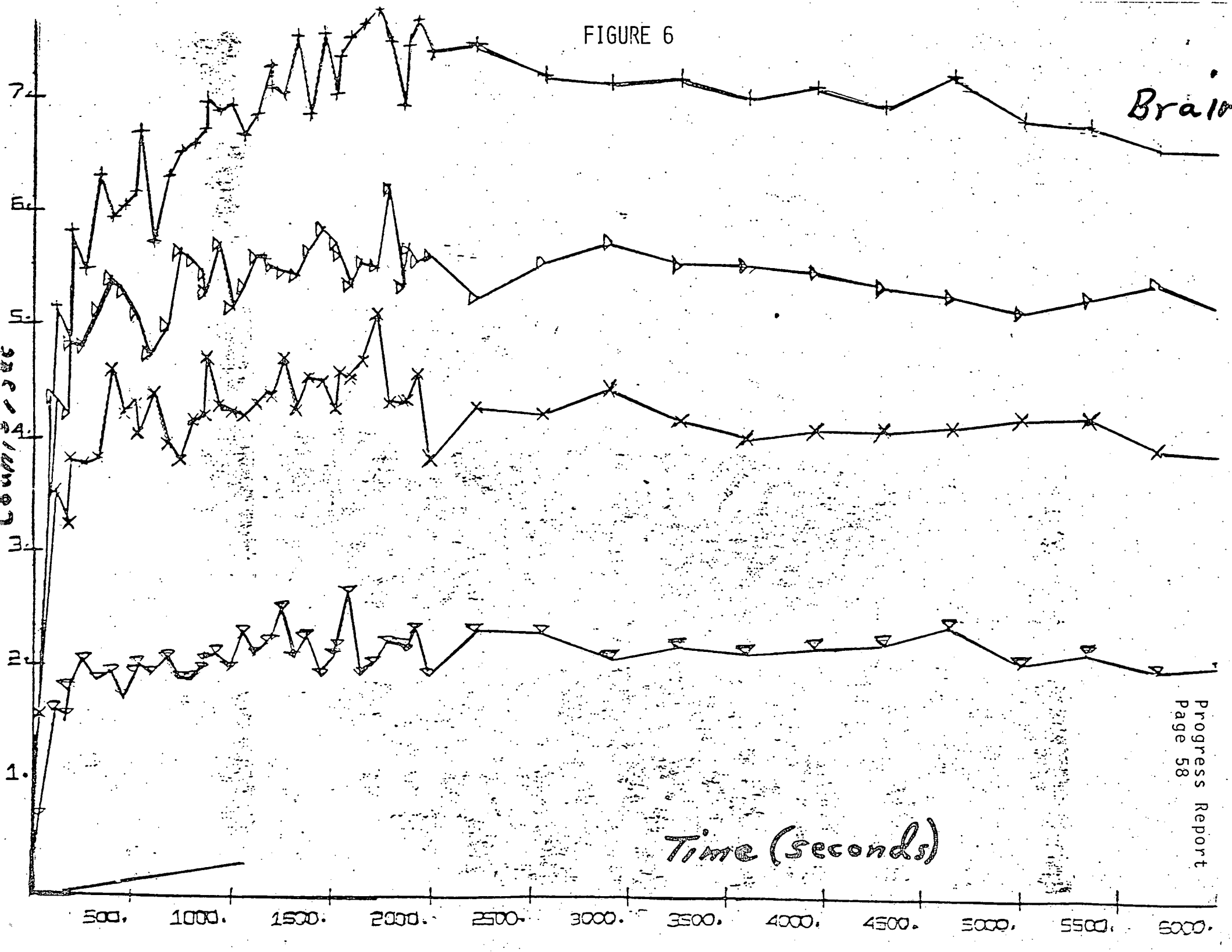
Brain
Time (seconds)
500.
1000.
1500.
2000.
2500.
3000.
3500.
4000.
4500.
5000.
5500.
6000.
1.
2.
3.
4.
5.
6.
7.

REFERENCES:

1. Janssen, P.A.J., Van de Westeringh, C., Jagenean, A.H.M., Demoen, P.J.A., Hermans, B.K.F., Van Daele, G.H.P., Schellekens, K.H.L., Van der Eyeken, C.A.M., and Niemegeers, C.J.E. J. Med. Pharm. Chem. I, 281, 1959.

2. Janssen, P.A.J. Recent advances in the butyrophenone series. Neuropsychopharmacol. 3:331, 1964.

3a. Soudyin, W., Van Wyingaarden, I. and Allewyn, F. European J. Pharmacol. 1:47, 1967.

b. Braun, G.A., Poos, G.I. and Soudyn, W. European J. Pharmacol. 1:58, 1957.

4. Kook, C.S., Reed, M.F. and Digenis, G.A. Preparation of (^{18}F) haloperidol. J. Med. Chem. 18:533-535, 1975.

5. Kook, C.S. Synthesis and *in vivo* distribution studies of (^{18}F) haloperidol and its major metabolite. Dissertation, 1975. University of Kentucky.

6. Tilbury, R.S., Dahl, J.R., Mamacos, J.P. and Laughlin, J.S. Fluorine-18 production for medical use by helium-3 bombardment of water. Int. J. Appl. Rad. Isotopes 21:277-281, 1970.

2.4 POTASSIUM-38 AS AN INDICATOR OF BLOOD FLOW TO THE MYOCARDIUM

As previously reported (1,2) we have developed a convenient method of producing 5 to 15 mCi amounts of potassium-38 with no added carrier in injectable saline.

Sapirstein (3) has shown that radioactive potassium-42 injected intravenously in rats is taken up by the heart to a maximum value in 10 seconds, remains the same for 60 seconds, and may be used as an indicator of blood flow to the heart. Poe (4) has compared the myocardial uptake and clearance characteristics of potassium and cesium, and showed that potassium remains at peak concentration between 5 and 20 minutes after I.V. injection, then clears with a half time of 6.5 hrs. Myers (5) pointed out that K-38 would be a better choice than K-43 for imaging the heart, because its 7.6 minute half-life closely matches the time of maximum uptake, and because it is a positron emitter. Also the radiation dose to the patient is greatly reduced as shown in Table 11, and repeat studies at about hourly intervals are possible.

In order to investigate the feasibility of studying the effect of drugs on blood flow to the myocardium the following experiments were performed in anesthetized dogs. About 5 mCi of potassium-38 as the chloride in isotonic saline was injected into a dog anesthetized with sodium pentabarbitol. The dog was scanned over the heart starting about 5 minutes after injection with the High Energy Gamma (HEG) scanner using the 511 keV gamma rays. The counts/minute/mCi of K-38 summed over the heart area, corrected for decay to the time of injection, were calculated. About 30 minutes later 0.5 mg/kg of the drug dipyridimole (Persantine, Boehringer-Ingelheim) was injected intravenously. Five minutes later K-38 was injected and about 10 minutes after that a HEG scan of the heart was performed. About one hour later another dose of K-38 was injected and the scan repeated. The scan was repeated again after a further one hour wait. The whole procedure was then repeated with different dogs using the drugs digoxin (1.5 mg/kg i.v., Lederle) and propranolol (0.2 mg/kg i.v., Inderal, Ayherst).

The results are shown in Table 12. Eight scans of pentobarbitalised dogs showed an average myocardial uptake of 12940 cps/mCi corrected to time of injection with a standard deviation of 11%. This was taken to be the normal range. It is seen that dipyridimole caused a 49% increase in K-38 uptake in the myocardium 19 minutes after injection and the uptake decreased to 36% after 1 hour and to within normal limits after 2 hours. This is consistent with the known pharmacological action of dipyridimole as a fast acting vasodilator causing blood flow to the myocardium to increase rapidly and decrease slowly back to normal within 3 hours.

Digoxin caused a slower rise of lesser magnitude which remained the same at 2.4 hours. Propranolol (0.2 mg/kg i.v.) caused no change in K-38 uptake, which is consistent with its effect of decreasing the heart rate and contractibility, and presumably not affecting blood flow.

TABLE 11

ESTIMATED RADIATION DOSES TO THE WHOLE BODY FROM VARIOUS RADIOPHARMACEUTICALS USED FOR MYOCARDIAL IMAGING, ARRANGED IN ORDER OF DECREASING DOSE

Radiopharmaceutical	Half-Life	Radiation Dose (rads/mCi)
K-42	12.4h	1.5
K-43	22 h	0.3
Co-129	32 h	0.14
Rb-81	4.7h	0.04
K-38	7.6m	0.012
$^{13}NH_4^+$	10 m	0.006

TABLE 12

K-38 HEART UPTAKE IN DOGS

Scan No.	MAI of Drug	Normalized Heart Activity cps/mCi at to
No Drug		
174	---	12,377
175	---	11,110
182	---	14,658
183	---	15,487
184	---	13,059
185	---	12,972
186	---	12,010
187	---	11,831
		12,938 ± 1474 = Average ± SD.
With Dipyridimole		
176	19	19,300
178	70	17,560
180	130	13,769
With Propranolol (Inderal)		
195	--	12,429
197	15	12,733
199	75	11,361
201	130	13,013
With Digoxin		
219	--	13,423
220	39	15,895
220	140	16,108

MAI = minutes after injection

*Normalized heart activity = normalized for number of scan elements.

REFERENCES

1. Tilbury, R.S., Dahl, J.R., Chandra, R. et al. Cyclotron production of potassium-38 for medical use. Proceedings of 2nd International Symposium of Radiopharmaceuticals Chemistry, Oxford, U.K., July 3, 1978, Paper 61. To be published in J. of Labeled Compounds & Radiopharmaceuticals.

2. Myers, W.G., Tilbury, R.S., and Dahl, J.R. Potassium-38. A 7.63 minute positron emitter for radio indicator studies in biomedicine. Proceedings of World Federation of Nuclear Medicine and Biology, September 17, 1978, Washington, D.C., USA.

3. Sapirstein, L.A. Regional blood flow by fractional distribution of indicators. Am. J. Physiol. 193 (1):161-168, 1958.

4. Poe, N.D. Comparative myocardial uptake and clearance of potassium and cesium. J. Nucl. Med. 13:557-560, 1972.

5. Myers, W.G. Radiopotassium-38 for in-vivo studies of dynamic processes. J. Nucl. Med. 14:359-360, 1973.

3. DOSIMETRY FOR INTERNALLY DEPOSITED ISOTOPES IN ANIMALS AND MAN

OBJECTIVE

To evaluate the radiation hazard associated with the use of radionuclides and labeled compounds in animals and man and thereby help make an early evaluation of proposed compounds for particular intended purposes.

SCOPE OF INVESTIGATION

A key ingredient in the intelligent choice of a radionuclide or labeled compound for any proposed use in humans is an evaluation of the radiation hazards associated with its use. Such evaluation normally begins with an analysis of the existing metabolic data for a preliminary radiation dose estimate. Where such data is lacking, specific studies of the distribution and dynamics of the agent of interest are initiated in selected model systems to provide the parameters required for radiation dose estimates.

RESULTS AND CONCLUSIONS

Two agents, ^{18}F-fluoroestradiol and ^{18}F-haloperidol, are in need of careful dosimetric evaluation. This work is in progress. The initial animal studies which have been completed at this time for these two agents are reported in other parts of this report. When possible preliminary radiation dose estimates will be made and updated as more information becomes available.

A compartmental model program called BIOSIM was obtained from the University of Pennsylvania. This program was designed for operation on large IBM systems (IBM 360) and is currently being modified by our group to operate on our new Control Data Corporation PDP 11/70 computer. This program uses experimental data directly in its search for the best fits and the model being tried may be very easily modified as the computer simulation process progresses. When operational this program will considerably improve our dosimetry estimates. Two other programs SAAM-27 (Simulation, Analysis, and Modeling) prepared as MED-17 and MIRD-S, a computer program to determine cumulated activity and radiation absorbed dose, prepared as MED-16-MIRD-S, have been obtained on magnetic tape through the Biomedical Computing Technology Information Center (BICTIC) at Oak Ridge National Laboratory. Both programs will require considerable modification in order to bring them into use on our PDP 11/70 computer.

A study titled, "Relationship of External Radiation Doses to Internal Dosimetry" was published as a chapter in a book, Therapy in Nuclear Medicine during the period of this report (1).

REFERENCE

1. Bigler, R.E. Relationship of external radiation doses to internal dosimetry. In: Therapy in Nuclear Medicine, Spencer, R.P. (Ed.), New York, Grune & Stratton, pp. 17-31, 1978.

4. INSTRUMENTATION AND ANALYTICAL PROCEDURES

4.1. CYCLOTRON RESEARCH AND DEVELOPMENT

OBJECTIVE

To maintain and improve cyclotron operating efficiency and reliability, to improve personnel and equipment safety and protection, and to simplify and standardize cyclotron operation.

SCOPE OF INVESTIGATION

The research programs utilizing the Sloan-Kettering cyclotron demand a high degree of cyclotron reliability and versatility, especially when patient scheduling is involved. Different particles and different beam currents on tight scheduling require daily and half-daily particle change over and cyclotron retuning, much more so than similar cyclotrons in other institutions. Also, the limited particle energy of our cyclotron requires long term stable high and low beam currents for production of some isotopes and neutrons. To meet these demands we have concentrated on developing simple and standard cyclotron operation and maintenance methods, stable and reproducible beam currents, optimum extraction efficiencies and extended life times for perishable components.

RESULTS AND CONCLUSIONS

1. Inner Orbits Correction

The quality and quantity of the internal beam and its effect on extraction efficiency and external beam depends on the configuration of the first turn and subsequent inner orbits, which in turn depend heavily on the positioning of components of the central region: the ion source, puller, first turn shield and dees. We have found that changes in position or dimensions of 0.010" in many of these components will cause substantial differences in cyclotron performance. In addition, these parameters are a compromise between those necessary for maximum proton, He-3, He-4, and deuteron operation. A system of harmonic coil magnets are used to alter the phase space of the beam entering the deflector and thus this system forms an important component of the external beam extraction system. Similar sets of coils installed close to the inner orbits of our cyclotron will increase extraction efficiency substantially by compensating for particle differences, correcting positional variances and providing additional tuning. Increase extraction efficiency will also lessen deflector loading, lengthening the period between servicings and thus reduce cyclotron staff radiation exposure levels. We have completed the design, fabrication and installation of a three sets of inner coils and are awaiting delivery of the necessary power supplies. Although this involved removal of major internal cyclotron components, the work was scheduled and spaced so as not to interrupt the research program.

2. Alpha-Particle Facility

Research programs involving accelerated alpha (He-4) particles have been greatly expanded. Connecting a gas cylinder to a spare gas sampling port when He-4 was needed became too cumbersome and inherently error-prone for routine operation. A He-4 facility was designed and installed in the gas delivery system to allow standard push-button operation interlocked with our other three gases.

3. Cyclotron Operation, Maintenance and Safety

The ions accelerated in our cyclotron are ionized gases generated in plasma arcs between cathodes in an ion source. These arcs erode the cathodes, which must be routinely replaced. The most rapid erosion is experienced with the ∿500 watt He-3 high arc, which has limited the cathodes to 25-30 hours of cumulative operation. We have rebuilt the cyclotron gas handling system, modified the flexible connection between the gas cart and cyclotron and modified the He-3 liquid nitrogen trap servicing procedure to reduce the impurities in the ion source gases. This has extended the He-3 high arc life of the cathodes routinely to 60-70 hours (a factor of 2 improvement).

Due to personnel changes and increased need for coordination of the cyclotron schedule with patient availability, heavy emphasis has been placed on training additional cyclotron operators, involving additional members of our current staff in this activity. Since January 1, 32 two-hour training sessions have been completed involving four new operators. By January this program is expected to result in one general purpose operator and three single particle operators.

A special 1-1/2 hour safety training program has been initiated, to instruct new personnel in all aspects of safety in the cyclotron facility (see Appendix A). Emphasis has been placed on demonstration and actual handling of the safety devices and each trainee receives a personal copy of our safety manual. Nine new staff and volunteers have been instructed since March, 1978.

APPENDIX A

SAFETY TRAINING I

A. Radiation Protection

1. Brief introduction to the cyclotron
2. Hot areas of the cyclotron: deflector, mag. channels, probe and target.
3. Use of the Jordan Radgun: demonstration and trainee handling.
4. Area monitors, film badges, dosimeters, Rad-Tads and survey meters.
5. Personnel Monitoring Station: survey meter, disposable boots and gloves.
6. Allowed radiation levels.

B. Irradiation Protection

1. "Scram" buttons: explanation, demonstration and handling.
2. Shielding door interlock and scram button and door interlock bypass: warning whistles for each.
3. "Anode On" illuminated warning sign.
4. Shielding door operation, door crush pads, manual opening tools and demonstration.
5. "Short Snorter" emergency air pack: demonstration and handling.
6. Special air conditioning in the facility.

SAFETY TRAINING II

A. Fire

1. Control console and SC-2 cyclotron power circuit breakers.
2. CO_2 fire extinguishers: locations and demonstration.
3. A, B and C fire types; C type power supply fire has happened several times.
4. Fire alarm box location and fire report extension 7979.
5. Expected smoke paths in facility.

B. Medical Emergency

1. Medical emergency extension 6000: all emergencies, connects directly with hospital emergency team.
2. CPR course: free and given at Center.
3. Unusual Occurance Report Form.

C. Radioactive Material Spills

1. Isolate area.
2. Call Medical Physics extension 7391.

D. Transporting and Handling Materials and Equipment

1. Shielding door track channel fillers.
2. Diamond plate handle recess fillers.
3. Safety shoes: supplied by the Center.
4. Eyewash station: location.
5. Compressed gas cyclinders: hazards and proper transporting and anchoring.

4.2 POSITRON TOMOGRAPHIC IMAGING WITH THE TOKIM SYSTEM

OBJECTIVE:

To implement and evaluate modifications to the TOKIM system which will improve its tomographic capabilities. These include collimator design, software development and studies with graded filters.

SCOPE OF INVESTIGATION:

Most of our effort in this contract period has been devoted to improving the computer software used in reconstrucing the focal plane images on the IBM 1800 computer and to transferring some of these algorithms to the PDP 11/70 computer. The software implementations have included:

1. A flexible method for convolving planar images in real space with Gaussian-shaped blurring functions for use in the iterative blurring and subtracting reconstruction routine.

2. The use of a band-reject filtering algorithm described by Stokely and Parkey (Proc. Fourth Internat. Conf. on Information Processing in Scintigraphy, Orsay, 1975, pp. 164-173) for removing the grid artifact introduced by the aperture-limiting "egg-crate" collimator.

3. The development of a reconstruction algorithm based on a probabilistic model.

RESULTS AND CONCLUSIONS:

The iterative reconstruction algorithm which was chosen to obtain the focused planar images requires convolving the 64 X 64 projection images with Gaussian filter functions whose "width" is related to the distance between the focal plane being reconstructed and each projection image. For large coincidence apertures, these filter functions could be quite large and a real-space convolution filter might include almost as many elements as the 64 X 64 image. Application of such large filters proved to be excessively time-consuming on the IBM 1800 (which has no floating-point hardware), and an alternative method is now used: a Gaussian random number generator produces a set of normally-distributed x and y displacements with a mean of 0.0 and a standard deviation appropriate to the width of the filter function. If the number of counts in an image element (i,j) was n, then the random number generator is applied $2n$ times and the n counts are "redistributed" into neighboring matrix elements according to the calculated x-y displacements.

This calculation is repeated (non-recursively) for each of the 4096 matrix elements and the resulting image smoothed lightly to reduce the effects of random noise introduced by the x-y displacement calculation. The method has the following advantages:

a) The filter is described by a single parameter (the standard deviation) and hence large amounts of core are not required to store the filter.

b) The execution time is a function of total counts in the image and hence the algorithm is fast in regions of the image where the count-rate is low, as opposed to fixed-size filters where execution time is the same for all picture elements.

c) Much of the arithmetic can be peformed in integer mode.

The band-reject filter algorithm was found to be effective in reducing the magnitude of the periodic "grid" artifact" produced by the egg-crate collimator. First, an algorithm which calculates the power spectrum of the image along a particular x or y coordinate enables the operator to correctly select the frequency band to be rejected (see Figure 7). Next, the filter is applied horizontally and vertically to the image in real space. Figure 8 shows the original unprocessed image of a square source of activity in the coincidence mode, along with the distribution after one and two passes with the band-reject filter. Note how the cross-hatched "bar" pattern has been reduced in magnitude by application of the filter.

In coincidence imaging with the TOKIM, each coincident event is recorded as two pairs of x-y coordinates which describe the intersection of the rays with the crystal planes of the detectors. This is sufficient to describe a line along which the event could have originated, but cannot supply information on the exact point of origin. However, the probability that an event originated at a given plane must be related to the actual activity distribution in the subject at the point corresponding to that plane; i.e. areas with higher activity densities will be those areas from which most of the line pairs will originate. An algorithm was written for the IBM 1800 which performs the following calculation in real space:

a) For each ray, a plane of "origin" is randomly assigned using a uniform random number generator.

b) The resulting "distribution," which represents the best approximation to the unknown real activity distribution, is used in Baye's Formula to compute the a priori probability that a given ray originated from a specific plane along the line. Other variables in the formula involve the point-spread functions of the planes of interest projected onto the crystal faces.

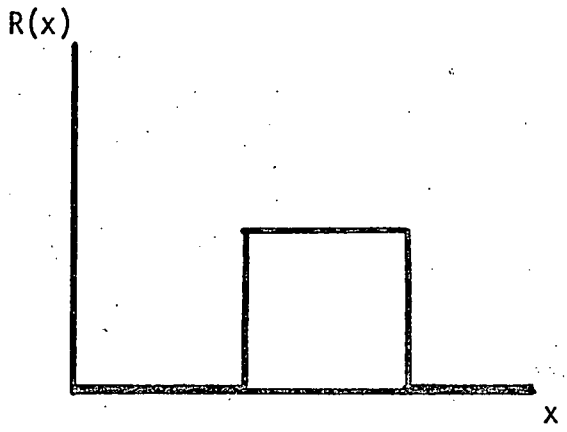

Real Activity Distribution

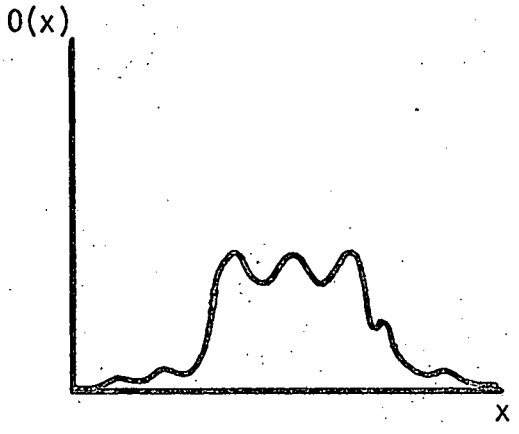

Observed Distribution with Grid Pattern

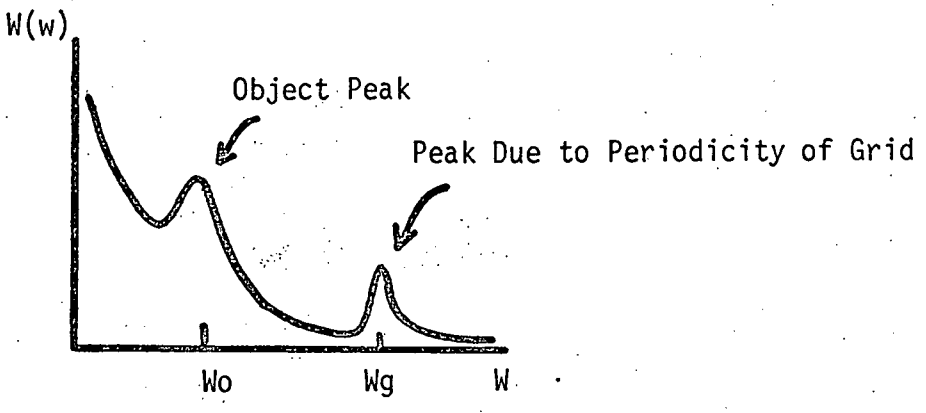

Figure 7 - Power Spectrum Calculation for Band Reject Filtering

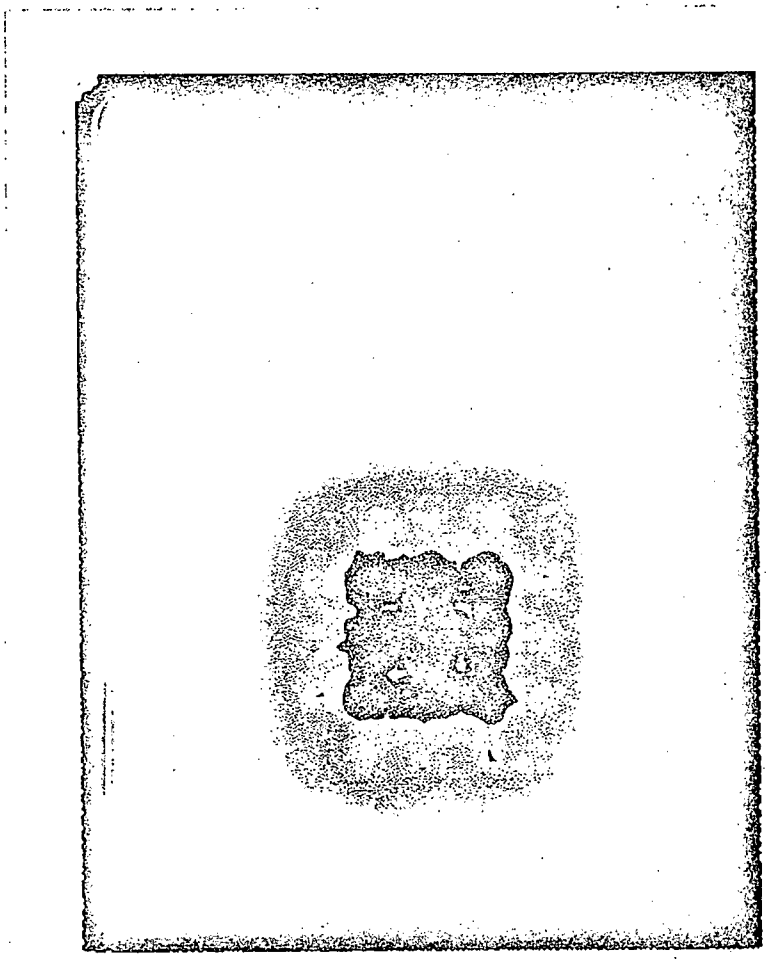

FIGURE 8a

Observed activity distribution of a square source of ^{68}Ge when imaged with the TOKIM in coincidence mode. 32 equal levels of intensity are displayed, with the resulting image multicycled. The reduction in intensity caused by absorption in the egg-crate pattern is clearly visible.

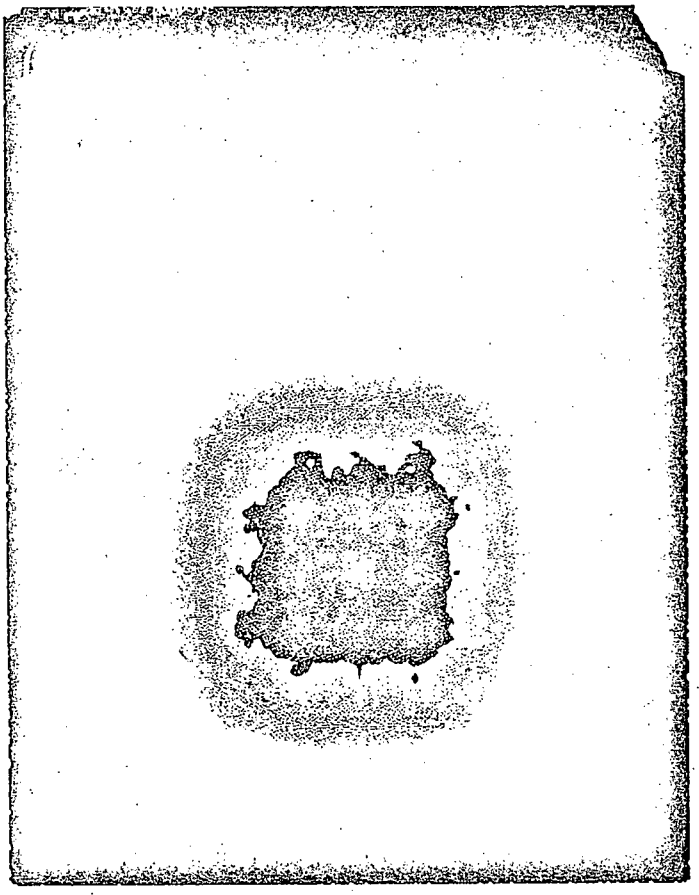

FIGURE 8b

The image in Figure 8a after one application of the digital band-reject filter.

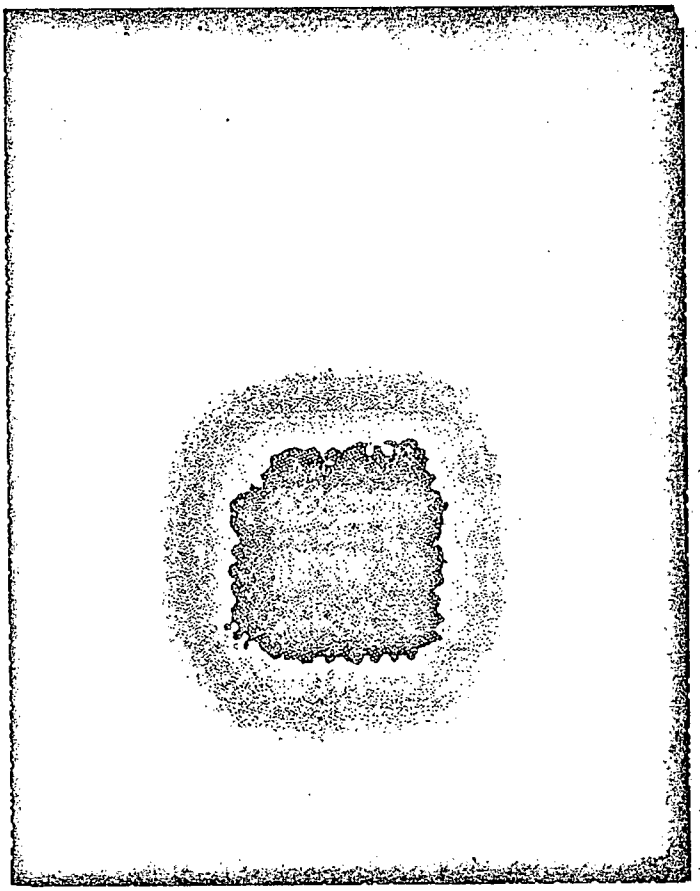

FIGURE 8c

The image after two applications of the filter. While still visible, the grid artifact is greatly reduced in intensity.

c) The plane which yields the maximum a priori probability for the ray is chosen as the new plane of "origin." This calculation is repeated for each ray in the image.

d) Steps b) and c) are repeated interatively until the reconstruction converges.

Preliminary experience with reconstructions on a point source indicate the following:

a) This reconstruction converges more rapidly than the blurring-subtracting algorithm.

b) Each iteration requires a great deal of execution time due to the heavy use of floating-point arithmetic and processing time is proportional to the total number of rays in the image.

c) The algorithm may be unacceptably susceptible to high-frequency noise as presently implemented. However, smoothing and thresholding techniques may overcome this problem.

In conclusion, it would appear that the following configuration of hardware and software would be most useful for the TOKIM in the tomographic mode: use of the egg-crate collimator and Muehllehner-type graded filters to reduce the coincidence aperture and the singles rate; use of the iterative blurring and subtraction algorithm to remove off-plane contributions from the longitudinal sections and use of the digital band-reject filter to compensate for the grid artifact introduced by the egg-crate collimator.

4.3 REVIEW OF POSITRON EMISSION TRANSAXIAL TOMOGRAPH INSTRUMENTS

The objective of this section is to review the design details for two commercially available proposed positron emission tomographic (PET) designs: ORTEC ECAT with a multislice option, and The Cyclotron Corporation PC 4500. Both proposed instruments are multiple-slice imaging units and can be used for any body region.

ORTEC has been manufacturing nuclear instrumentation modules and systems for over 20 years. Their experience in analyzing state-of-the-art electronics for nuclear research is extensive. As a basis for the ECAT, ORTEC started by using a proven PETT III design developed by the St. Louis group. They upgraded the computer configuration to a standard well-defined multi-user system, upgraded the mechanical design, and developed a standard modular electronic package. The proposed multislice ECAT will consist of one additional plane of detectors using the same basic electronic hardware, computer configuration, and software as the single slice version. The additional detector plane will enable the reconstruction of three slices, the center slice of which includes cross coincidences between detector planes. Projected resolution specifications of this device are essentially those of the single slice device.

The basis for the first Cyclotron Corporation positron camera tomograph was the prototype PC II developed by Dr. Gordon Brownell at the Massachusetts General Hospital. The PC 4200 uses the original PC II design with improvements and modifications in the mechanical design of the gantry, the electronic hardware, and the computer system (the PC 4200 is currently on loan to MSKCC for evaluation and testing). The PC 4500 proposed design as currently designated consists of five circular planes of 88 detectors each. The electronic hardware and the computer configuration are similar to the PC 4200.

The comparative technical specifications of the two currently available total body transaxial computed tomographic instruments are summarized in Table 13.

TABLE 13

SUMMARY OF CURRENTLY AVAILABLE POSITRON TOMOGRAPH SPECIFICATIONS

SPECIFICATION	ORTEC: MULTISLICE ECAT	CYCLOTRON CORPORATION: PC 4500
Number and arrangement of NaI (Tl) crystals	Two banks of 66 crystals arranged hexagonally	Five rings of 88 crystals
Crystal dimensions	Each crystal cylindrical, 28.1 mm wide x 76.2 mm deep	Cylindrical, 2 cm diameter, 6 cm long
Intercrystal spacing	Crystals are 45.7 mm apart center to center, therefore 7.6 mm separate adjacent crystals	2.8 cm center to center
Interplane shielding	1.5 inch of lead outside of planes with a lead septum used to separate planes	2.8 cm center to center for "straight across" planes, 1.4 cm center to center including "cross plane" slices
Number of planes along z axis	Three slices will be imaged simultaneously	Five straight across, 4 cross plane, 9 total
Provisions for changing shielding configuration	Shadow shields, which define the spatial resolution are changeable	Shielding could be optimized for head only, or head and body applications
Field of view	50 cm field of view, with detector faces 100 cm apart	36 cm diameter + 2.8 cm wobble
Patient opening	50 cm patient opening	50 cm
Detector motion	Detector banks translate in 8 steps of 0.57 cm or 4 steps of 1.14 cm and rotate in 5°, or 10° steps	Tilt and wobble
Angular measurements	Angular samplings are made in 2.5° segments	Fully programmable

SUMMARY OF POSITRON TOMOGRAPH SPECIFICATIONS (CONT'D.)

SPECIFICATION	ORTEC: MULTISLICE ECAT	CYCLOTRON CORPORATION: PC 4500
Minimum time required for complete scan	10 seconds live time (minimum)	Approximately 2 seconds per tilt position 3 tilt positions, approximately 8-10 seconds for a full scan. Note: sampling pattern is completely flexible and programmable and is not fixed
Resolution characteristics (in the plane)	Guaranteed: 20 mm without shadow shields 15 mm with standard shadow shield 12 mm with high resolution shadow shields Typical: 18 mm 13.5 mm 10 mm	1 cm FWHM
Sensitivity characteristics	Slices number 1 and 2 have efficiency of $\geq$ 12,500 c/sec/μCi/ml @ Standard shields $\geq$ 24,000 c/sec/μCi/ml @ Shields removed Center projected to have approximately 1.9 times these efficiences	16,000 CPS/μCi/cm^3 (straight across plane) 32,000 CPS/μCi/cm^3 (cross plane) 2 x 10^5 CPS/μCi/cm^3 (total system) with 20 cm diameter water filled phantom
Z axis resolution	Without shadow shields, 18.5 mm ± 1.0 Standard shadow shields, 19.5 mm ± 1.0 High resolution shadow shields, 21.0 mm ± 1.0	1 cm FWHM

SUMMARY OF POSITRON TOMOGRAPH SPECIFICATIONS (CONT'D.)

SPECIFICATION	ORTEC: MULTISLICE ECAT	CYCLOTRON CORPORATION: PC 4500
Resolution in 2 dimensional rectilinear mode	With standard shields and high resolution reconstruction approximately 15 mm, other choices at user's option	1 cm FWHM
Coincidence time resolution	$\leq$ 12 nanoseconds (approximately)	20 nanosec timing
Random coincidence correction	Three modes, operator electable: A) Increment totals, ignore randoms. B) Increment totals, decrement randoms C) Increment totals, route randoms to separate memory	Design not frozen yet
Type of discriminator	Constant fraction	Proprietary
Computer manufacturer/model No.	DEC PDP 11/60, RSX-11M	PDP 11/34, RT-11
Memory	128K MOS Memory (standard)	32 K Words
Price (Estimate)	$650,000 F.O.B. Oak Ridge, Tenn.	$750,000
Delivery Time (Estimate)	9-11 Months ARO	1 Year ARO

PUBLICATIONS Oct. 1977 - Sept. 1978

1. Bigler, R.E. Relationships of external radiation doses to internal dosimetry. In: Therapy in Nuclear Medicine, Spencer, R.P. (Ed.), New York, Grune & Stratton, 1978, pp. 17-31. (Invited Paper, presented March 17-19, 1978, Hartford, Connecticut).

2. Bigler, R.E., Kostick, J.A., Davis, D.C., Russ, G.A., Hopfan, S., Tilbury, R.S. and Laughlin, J.S. The use of $C^{15}O$ and $^{15}O_2$ steady-state imaging to monitor radiation treatment effects. IEEE Transactions on Nuclear Science, NS25, #1, 174-179, 1978. (Presented at the 1977 IEEE Symposium on Nuclear Science, San Francisco, October 19-21, 1977).

3. Bigler, R.E. Total-body calcium by the Ar-37 method: current feasibility status. Applied Radiology 7:149-152, 1978. (Invited Paper).

4. Cooper, A.J.L., McDonald, J.M., Gelbard, A.S. and Duffy, T.E. Metabolic fate of ^{13}N-labeled ammonia in rat brain. Trans. Am. Soc. Neurochem. 9:187, 1978. (Abstract)

5. Gelbard, A.S. and Cooper, A.J.L. Synthesis of ^{13}N-labeled aromatic L-amino acids by enzymatic transamination of ^{13}N-L-glutamic acid. Second Internat. Symp. Radiopharmaceutical Chemistry, Oxford, England, p. 94, Sept., 1978. (Abstract)

6. Gelbard, A.S. N-13-L-Amino acids, synthesized enzymatically, for in-vivo metabolic studies. Second Internat. Congress of the World Federation of Nuclear Medicine & Biology, Washington, D.C., p. 3, Sept. 1978.

7. Kuo, T.Y.T. and Laughlin, J.S. Improvement in beam current performance of the biomedical cyclotron at Memorial Sloan-Kettering Cancer Center. Proc. 4th Medical Cyclotron Users Conf., March, 1976. In: Progress in Nuclear Medicine, S. Karger, Basel, Switzerland, Vol. 4, 6-15, c1978.

8. Lockwood, A.H., McDonald, J.M., Reiman, R.E., Gelbard, A.S., Laughlin, J.S., Duffy, T.E. and Plum, F. The dynamics of ammonia metabolism in man. Gastroenterology 73:1232, 1977.

9. Tilbury, R.S. The Memorial Sloan-Kettering biomedical cyclotron facility: Program overview. In: Progress in Nuclear Medicine, S. Karger, Basel, Switzerland, Vol. 4, pp. 2-5, c1978.

10. Tilbury, R.S. The Memorial Sloan-Kettering biomedical cyclotron facility: Radioisotope production and labeled compounds. In: Progress in Nuclear Medicine, S. Karger, Basel, Switzerland, Vol. 4, pp. 100-107, c1978.

IN PRESS

1. Cooper, A.J.L., McDonald, J.M., Gelbard, A.S., Gledhill, R.F. and Duffy, T.E. The metabolic fate of ^{13}N-labeled ammonia in rat brain. J. Biol. Chem., 1978. (In Press)

2. Myers, W.G., Tilbury, R.S. and Dahl, J.R. Potassium-38. A 7.63 minute positron emitter for radio-indicator studies in biomedicine. Proc. World Federation of Nuclear Medicine & Biology, Washington, D.C., Sept. 1978. (Abstract)

3. Tilbury, R.S., Dahl, J.R., Chandra, R., McDonald, J.M., Reiman, R.E. and Myers, W.G. Cyclotron production of potassium-38 for medical use. Proc. 2nd Internat. Symp. on Radiopharmaceutical Chemistry, Oxford, England, July, 1978. (Abstract) In Press J. Labeled Compounds & Radiopharmaceuticals, 1978.